763
c

DETERMINATION OF NUCLIDIC RATIOS IN GEOLOGICAL SAMPLES WITH NEUTRON CAPTURE GAMMA RAYS

DETERMINATION OF NUCLIDIC RATIOS IN GEOLOGICAL SAMPLES WITH NEUTRON CAPTURE GAMMA RAYS

by

M. A. ISLAM

A Thesis

Submitted to the School of Graduate Studies

in Partial Fulfilment of the Requirements

for the Degree

Master of Science

McMaster University

June 1979

MASTER OF SCIENCE (1979)
(Physics)

McMASTER UNIVERSITY
Hamilton, Ontario

TITLE: DETERMINATION OF NUCLIDIC RATIOS IN GEOLOGICAL SAMPLES WITH NEUTRON CAPTURE GAMMA RAYS

AUTHOR: M.A. Islam

SUPERVISOR: Dr. W.V. Prestwich

NUMBER OF PAGES: ix, 99

SCOPE AND CONTENTS:

This thesis is divided into two parts, the first part being devoted to the application of Neutron Capture Gamma Ray Analysis in determining S/Si and Fe/Si ratios in Allende meteorite and lunar samples and the second part, to evidence for a possible iron isotopic anomaly in the Allende meteorite obtained by the same method. The samples were irradiated in an in-core irradiation system in the McMaster swimming-pool nuclear reactor and the collimated beam of gamma rays was detected by a pair-spectrometer consisting of a Ge(Li) detector and NaI annulus. In the first part, besides the mainstream of the work, the basic principles of Neutron Capture Gamma Ray Analysis and Neutron Activation Analysis and the supremacy of the former over the latter for this particular problem has been discussed. In the second part, along with the implications and evidence of isotopic variations of other elements in the Allende meteorite, a brief description of the classification, structure and mineralogy of the Allende meteorite is given. The success and advantage of the method along with its limitations and further directions along these lines are also discussed.

ACKNOWLEDGEMENTS

I would like to express my sincere thanks to my supervisor Dr. W.V. Prestwich whose guidance, inspiration and invaluable assistance made the completion of this work much easier. I wish to thank Dr. T.J. Kennett for his help and counsel. I am especially indebted to Dr. C.E. Rees for continued helpful discussions and assistance. I thank Dr. H.G. Thode for kindly supplying the Allende and the lunar samples. I also acknowledge the help and co-operation of Mr. C. Adesanmi, Mr. N. Barkman, Dr. P. Brewster, Mr. K. Chin, Dr. S. Kerr and Dr. Z. Top. My appreciation goes to Mrs. D. Matthews for typing the manuscript nicely. Finally, I would like to thank my wife Nasima for her moral support and encouragement during the course of this study. I also appreciate her help in the preparation of this manuscript and I dedicate this work to her.

TABLE OF CONTENTS

LIST OF ILLUSTRATIONS

LIST OF TABLES

PART I

ELEMENTAL RATIO DETERMINATION IN GEOLOGICAL SAMPLES WITH NEUTRON CAPTURE GAMMA RAYS

CHAPTER I

INTRODUCTION

1.1 NEUTRON CAPTURE PROMPT GAMMA-RAY ANALYSIS

A low energy neutron, being electrically neutral, can approach a nucleus without repulsion and once within range of the nuclear force, it is strongly absorbed. The target nucleus increases by unit mass number and it becomes a compound nucleus with excitation energy equal to the sum of the single neutron separation energy and the kinetic energy of the incident neutron. The compound nucleus may de-excite with the ejection of a nucleon or a light nucleus or with the emission of a single photon or several photons in cascade. This work is concerned with the one involving photon emission.

The emitted photons have energies characteristic of the emitting nuclides and thus can be utilized for the detection or measurement of the corresponding elements in the target material. This emission occurs with a typical lifetime of about 10^{-14} second and hence the photons are called prompt gamma rays. A method involving the spectrometry of these gamma rays can be a powerful tool in analytical science. Throughout this work this method

will be referred to as Neutron Capture Gamma-Ray Analysis and abbreviated as NCGA. In this work we shall determine certain elemental ratios in geological samples by NCGA.

1.2 COMPARISON WITH NEUTRON ACTIVATION ANALYSIS

Another similar method which is already applied widely in various fields of science and industry is Activation Analysis. The basic principle of activation analysis is that one or more of the stable isotopes of an element are converted into radioactive nuclides with suitable nuclear reactions e.g., bombardment with neutrons, charged particles or by high energy X-rays. The product nuclide can then be identified by its radiation, i.e. beta-particles and gamma-rays and by its half life. By using a comparison sample containing a known amount of a particular element and treating it in exactly the same way as the unknown specimen, the analysis can be made quantitative.

The majority of the activations are carried out with thermal neutrons from a reactor leading to the (n,γ) reaction and the method is then more specifically called Neutron Activation Analysis or briefly NAA. After the emission of prompt gamma-rays the product nuclide may be

radioactive. It may eventually beta decay with or without a gamma-ray. Beta decay without a gamma-ray is less preferable for the analysis because the beta spectrum often does not identify the emitter uniquely. The gamma-ray following the beta decay is often called a delayed gamma-ray contrasting the prompt one emitted during the de-excitation of the compound nucleus.

For this method to be suitable, the product must be radioactive and its half-life must be convenient for measurement, i.e. neither too long nor too short. Furthermore, the cross-section for neutron capture must be sufficiently large for the product to acquire adequate activity for measurement in a reasonable exposure time. These factors mainly set the limit to the mass for the detectability of the element.

Both the NCGA and NAA are non-destructive instrumental methods and bulk analysis is possible by both of them. No treatment of the sample is required prior to analysis. Prompt gamma analysis involves so few operations that the sources of variability are limited. For NCGA to be applicable, the cross-section for neutron absorption should not be too low and the

spectrum should be characterized by a suitable high intensity transition. It is obvious that while one method may not be applicable to a particular elemental analysis, the other may be. For this type of work, i.e. determination of elemental ratios, NCGA is often more suitable than NAA. In NAA one can find suitable pairs of elements less frequently because of the more stringent requirements involved. In addition to the neutron capture cross-sections for the pair of isotopes, the half-lives of the products are further constraints. Again, the irradiation conditions suitable for one element are often very unsuitable for another. There are timing errors which must be considered in activation analysis. High instantaneous counting rates are encountered, often due to radioisotopes in the matrix other than the one of interest. For determining the elemental ratios these problems are absent in NCGA.

1.3 MOTIVATION FOR THIS WORK

In the first part of this work the ratios of sulphur to silicon and iron to silicon have been determined for a lunar sample and the Allende meteorite by Neutron Capture Gamma Ray Analysis.

It is the sulphur analysis in the lunar sample which is of major concern. Chemical methods of determination of sulphur content have flaws especially where sulphur content is low. Chemical methods are chemical form dependent. There may be mechanical loss while weighing. The amount of sulphur content in the lunar sample as determined by chemical methods and reported by two groups (1), (2) differs by a factor of 1.5. Furthermore, in some cases, as in the case of the lunar sample which is extremely valuable, a non-destructive method is advantageous. Chemical methods are destructive.

Instrumental methods are chemical form-independent and can be non-destructive. Of course in NCGA, the sample becomes radioactive. Nevertheless it can be used for further research purposes in a few months after its irradiation, when the induced radioactivity has reduced to insignificant levels.

Since there are discrepancies in the reported values of sulphur content in the lunar sample determined by two different chemical methods, it was felt that a third method, preferably instrumental, should be applied to this problem.

In one instrumental method, X-ray fluorescence, sulphur has emissions which are soft and the radiation is easily attenuated by other matrix elements. Thus, this technique is not the proper choice for the determination of sulphur in the lunar sample.

It is difficult to detect sulphur with neutron activation analysis. The possible activation reactions are:

$^{32}S(n,p)^{32}P$	no γ,
$^{32}S(n,2n)^{31}S$	threshold : 16 MeV; $T_{1/2}$ = 2.64 S,
$^{34}S(n,\gamma)^{35}S$	no γ,
$^{34}S(n,\alpha)^{31}Si$	^{31}Si γ branching ratio .1%; interfered with by $^{31}P(n,p)^{31}Si$,
$^{36}S(n,\gamma)^{37}S$	σ = .146b; ^{36}S nat. ab. .014%; thermal n used,
$^{34}S(n,p)^{34}P$	^{34}S nat. ab. 4.2%; σ = .0756 b threshold : 14.5 MeV.

It is evident that the last reaction is the only good candidate for neutron activation analysis. But even

with this reaction, Gad Shani et al. (3) found the lower detectable limit of sulphur to be 100 mg. With the measurement of 100 mg of sulphur in the atmosphere the error was 26%. In the lunar sample in this work there was 1 mg of sulphur. This is far beyond the scope of neutron activation analysis.

Neutron Capture Gamma-Ray Analysis is a possible method for determining sulphur content in geological samples. Jurney et al. (7) discussed the possibility of determining low sulphur content in environmental sample by NCGA and they determined sulphur in orchard leaves to be .5 mg with a standard deviation of 13%. They used lines at 841 keV and 2380 keV which were favourable for their detection limit. Fay et al. (8), Rasmussen (9 to 11), Parsignault et al. (12) and Profio et al. (13) applied the same method for analysis of coal for sulphur.

It was decided to apply the method of NCGA to sulphur analysis in geological samples. The McMaster Nuclear Reactor and the Ge(Li) pair spectrometer is an excellent combination for carrying out work with NCGA. For the lunar sample, sulphur analysis might resolve the discrepancies in the existing reported values.

By NCGA, in principle, the concentration of an element can be determined in either of the three following ways:

(a) by determining the absolute mass of the element in a sample of known total mass,

(b) by adding known additional mass of the element of interest to the sample,

(c) by determining the ratio of that element to another element whose concentration is well-established in the literature.

With the facilities at McMaster the first method is very difficult to apply. This method involves the comparison of a transition line of the element in the sample with that of the same element with known mass in a standard sample. But this requires correction for variations in the neutron flux and the result depends on the geometry and irradiation position of the samples. Apart from neutron flux variation due to power fluctuations, the flux may also be dependent on the matrices of the sample. With facilities here, this method is either infeasible or feasible with great loss in accuracy.

The method of addition is a standard one and often used for analytical purposes. But when the concentration of an element of the sample is previously known, the third method is the simplest and particularly useful when addition of an element to the sample is not desirable. Since both the Allende and the lunar samples have limited supply they deserve repeated use. But altering the composition will obstruct further experiments with the same samples. Moreover, since silicon is a common component in most of the geological samples and its concentration is well-established for both the Allende and the lunar sample, (19 and 29), it was decided to choose the last approach.

Before proceeding to measure the sulphur to silicon ratio for the lunar sample, the same is at first determined for the Allende meteorite, a value which is well-established in the literature by other methods. Thus, at first the accuracy of the method is tested and then it is applied to the problem of the lunar sample.

As will be discussed in detail later on, the sulphur line is interfered with by a line of iron, which is a component of both the Allende and the lunar sample. For corrections, measurements on iron became necessary and this

opportunity is utilized to determine iron to silicon ratios for both the samples. These values are also cross-checked with the available values in the literature. In this way an independent verification of the silicon determination is possible.

For S, Si and Fe proper transition lines with high intensity and minimal interference are available for analysis. Sulphur has such a transition at 5420 keV with intensity around 60 per 100 captures (4 to 6). The transition line analyzed for silicon is at 3539.3 keV with intensity 79.58 per 100 captures (16). That for iron is the doublet (7631.6 and 7645.6 keV) with intensity 27.19 + 22.14 (16).

1.4 GAMMA RAY SPECTROSCOPY

Gamma-ray spectroscopy is a vast field which has been essentially the subject of a number of books. The question of its comprehensive discussion does not arise here. However a short discussion about two types of detectors, namely, the Ge(Li) and NaI(Tℓ) detectors will help the reader to appreciate the method of instrumentation applied and subsequently discussed in this work.

1.4.1 Ge(Li) SEMICONDUCTOR DETECTOR

A lithium-ion drifted germanium detector is essentially a modified n-p junction type detector. Normally, the main principle behind the n-p junction detector is to join an n-type semiconductor with a p-type and to create an intrinsic semiconductor layer between them by applying proper reverse-bias voltage. The detection of an ionizing particle and its energy measurement involves the entrance of the particle into the depletion region, creation of electron-hole pair by the former in the latter and subsequent collection of electrons and holes by the positive and negative electrodes. The pulse height obtained from the semiconductor detectors is proportional to the initial energy of the incident particle and the detectors have excellent resolutions. But since the depletion layer in the detectors is not more than a few millimeters, these devices can be used only for spectra of particles of low and moderate energies and thus do not make efficient gamma-ray detectors. This limitation has been overcome in the Ge(Li) detector.

The Ge(Li) detector was introduced by E.M. Pell in the United States in 1960 (41). Lithium, which acts

as an electron donor, is drifted into p-type germanium to produce an intrinsic region between the n- and p-regions. The lithium forms a stable chemical compound with the acceptor impurity which is boron. Thus a so-called p-i-n detector is formed with a much larger active volume. With the improvements in technique, active volumes up to 120 cm^3 have been manufactured and it has been possible to study spectra of gamma rays of high energy with these detectors.

1.4.2. NaI(Tℓ) SCINTILLATION DETECTOR

The phenomenon in which certain materials luminesce while exposed to nuclear radiations has been utlized in a powerful type of radiation detector called the scintillation counter. In this detector, the scintillations produced are converted to current pulses by a photoelectric cathode and a photomultiplier tube. The proportionality existing between the number of photons emitted and the energy deposited in the phosphor crystal by the gamma ray, makes this device useful for measuring the energy of the gamma ray.

The NaI(Tℓ) detector is such a scintillation counter in which NaI "activated" with small amounts of

thallium (typically 0.1% mole fraction) is used as a scintillator. Sodium iodide (with thallium) is a highly effective scintillator as far as light output is concerned. The presence of the element iodine, with a fairly high atomic number, gives it a large interaction cross-section for gamma rays; it is consequently, a very useful counter for high energy gamma radiation.

1.4.3 COMPARISON BETWEEN Ge(Li) AND NaI(Tℓ) DETECTORS

Although both of these detectors are suitable for the studies of gamma ray spectra, each one has a clear advantage over the other. Each of them has its own purpose and both of them comprise the pair-spectrometer used in this work. As only about 3 eV energy is needed to create an electron-hole pair in a Ge(Li) detector in contrast to 30 eV needed for producing a scintillation photon in sodium iodide, a Ge(Li) detector is intrinsically much higher in resolution than a NaI(Tℓ) detector. For example, our Ge(Li) detector gives a peak of a FWHM (full width at half maximum) of 2 keV at 1330 keV while the NaI(Tℓ) detectors are, on the other hand, much more efficient as NaI crystals can be made much larger than available Ge(Li) detectors. These detectors are extremely versatile as

they can be manufactured in different shapes and sizes and can be efficiently operated over a wide range of temperatures and under rugged handling conditions. Ge(Li) detectors have the drawback that they should be operated at very low temperatures. Liquid nitrogen (-196°C) has to be constantly used to cool the germanium semiconductor and to prevent the precipitation of the lithium complex.

CHAPTER 2

EXPERIMENTAL FACILITY

2.1 IRRADIATION SYSTEM

The McMaster swimming-pool nuclear reactor can provide a large flux density of neutrons for several purposes including neutron capture gamma ray analysis. It has a core loading capacity of 5.0 Kg of uranium enriched to 93% ^{235}U. Although it is capable of operation at up to 5 MW, it is usually operated at a power level of 1.0 MW thermal with an average flux of approximately $10^{13} n/cm^2/s$. The water of the pool serves the triple purpose of moderation, cooling and shielding.

In Fig. (1), the sample irradiation system is shown. Arrangements are such that there is a high flux density at the sample position while at the same time the intense background of gamma rays during fission and those emitted by structural elements of the core following neutron capture, are eliminated. As shown in the figure, a tangential through tube of aluminum with 7.62 cm inner diameter passes close to the reactor core and allows gamma rays from the sample to be extracted through a 1 cm stepped lead

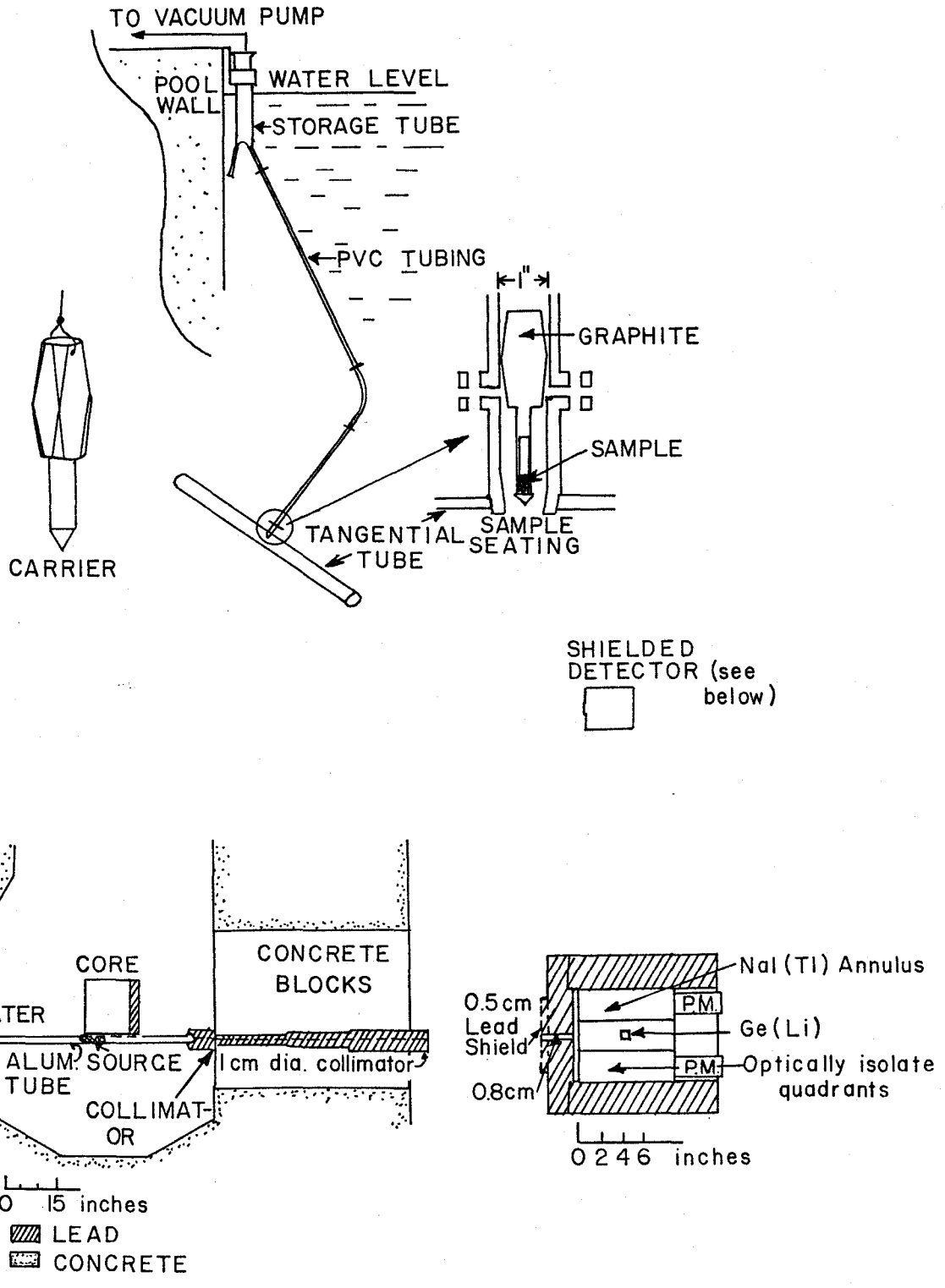

FIG. 1. THE IRRADIATION SYSTEM

collimator to a Ge(Li) detector. The beam is interrupted on its way by 50 cm of paraffin which removes fast neutrons and prevents radiation damage to the germanium crystal.

For inserting the sample into the irradiation position there is a flexible polyvinyl chloride tube 10 m long and 2.5 cm in diameter leading from the pool surface to the through tube which is below 8 m of water. Samples are placed in containers and lowered into position by means of nylon string and chains made of aluminum wire. After the sample is in, the sample insertion tube and through tube are evacuated to prevent background due to the (n,γ) reaction on nitrogen. As the sample may be appreciably radioactive for several hours after removal from the core, there is a storage location so that the sample may be stored underwater.

Carbon and beryllium capsules are most suitable as containers and both of them were used in this work. They have a few transition lines and they produce a minimum of background by the (n,γ) reactions. They do not remain too radioactive after removal from the core. Carbon and beryllium do not suffer significant radiation

damage while in the core. There was a low level of impurities in the material of the capsules and small corrections for the interference produced were made.

There are backgrounds of 2223 keV peak resulting from reaction $^{1}H(n,\gamma)^{2}H$ and also a peak at 7723.8 keV resulting from neutron capture in aluminum of the end plates of the through tube. This background, however, does not interfere with the peaks of interest in this work.

2.2 SPECTROSCOPY SYSTEM AND ELECTRONIC CIRCUITRY

The Ge(Li) detector in the simple mode has a complicated response function for photons with incident energy exceeding the pair creation threshold. The positron annihilation quanta may undergo Compton interaction and one or both of them may escape the detector. This will essentially give a continuum and three peaks corresponding to full energy, single-escape and double-escape of the quanta.

If only those events for which two 511 keV quanta leave the detector are accepted, the continuum due to Compton interactions, and the full-energy and single-escape peaks are suppressed. This is accomplished by surrounding

the Ge(Li) detector by a quadrisected NaI(Tℓ) annulus. Two quanta are simultaneously detected by either of the diametrically opposite pair of NaI(Tℓ) detectors. As in the high energy regions the double-escape peaks are by far the dominant ones, the suppression of the full-energy or single-escape peaks causes little loss of information of interest. However, as not all 511 keV photons will interact with the sodium iodide annulus in such a way that full energy will be left in the crystal, many double-escape photons will bypass detection. This loss of efficiency, however, is overcompensated by the increase in peak to background ratio.

The pair-products, the electron and positron, during the stopping process, will give bremsstrahlung photons which might escape the central detector. This effect gives an increasing continuum before the peak with a dip just before it. The dip is due to the inability of low energy bremsstrahlung photons to escape the detector. Events involving escaped bremsstrahlung photons can be partially suppressed by a simple logic circuitry. If the diametrically opposite quadrants detect two 511 keV photons and a third quadrant receives a photon of more than 50 keV, the event

is rejected. The threshold of 50 keV is chosen in order to avoid possible cross-talk between adjacent quadrants via the approximately 30 keV X-rays from iodine and also because the probability for escape of 50 keV quanta from the central detector is practically negligible.

Because of the inherently poor resolution of NaI(Tℓ) detectors, photons of energy slightly lower than 511 keV will be detected by the quadrant pair. These are the 511 keV photons which left some energy in the central detector. This results in a high energy "toe" on the peaks. Since this is an inherent problem with the NaI(Tℓ) detector, this situation cannot be improved with these devices.

The electron or positron or both may escape the active region of the detector and this range effect will give a continuum from 0 to $E-2moC^2$. This was not corrected for in this work. This and some more corrections are, however, possible by some more electronic arrangements and for its discussion and also for more complete discussions of the above, the reader is referred to Colenbrander and Kennett (14) and Robertson et al. (15).

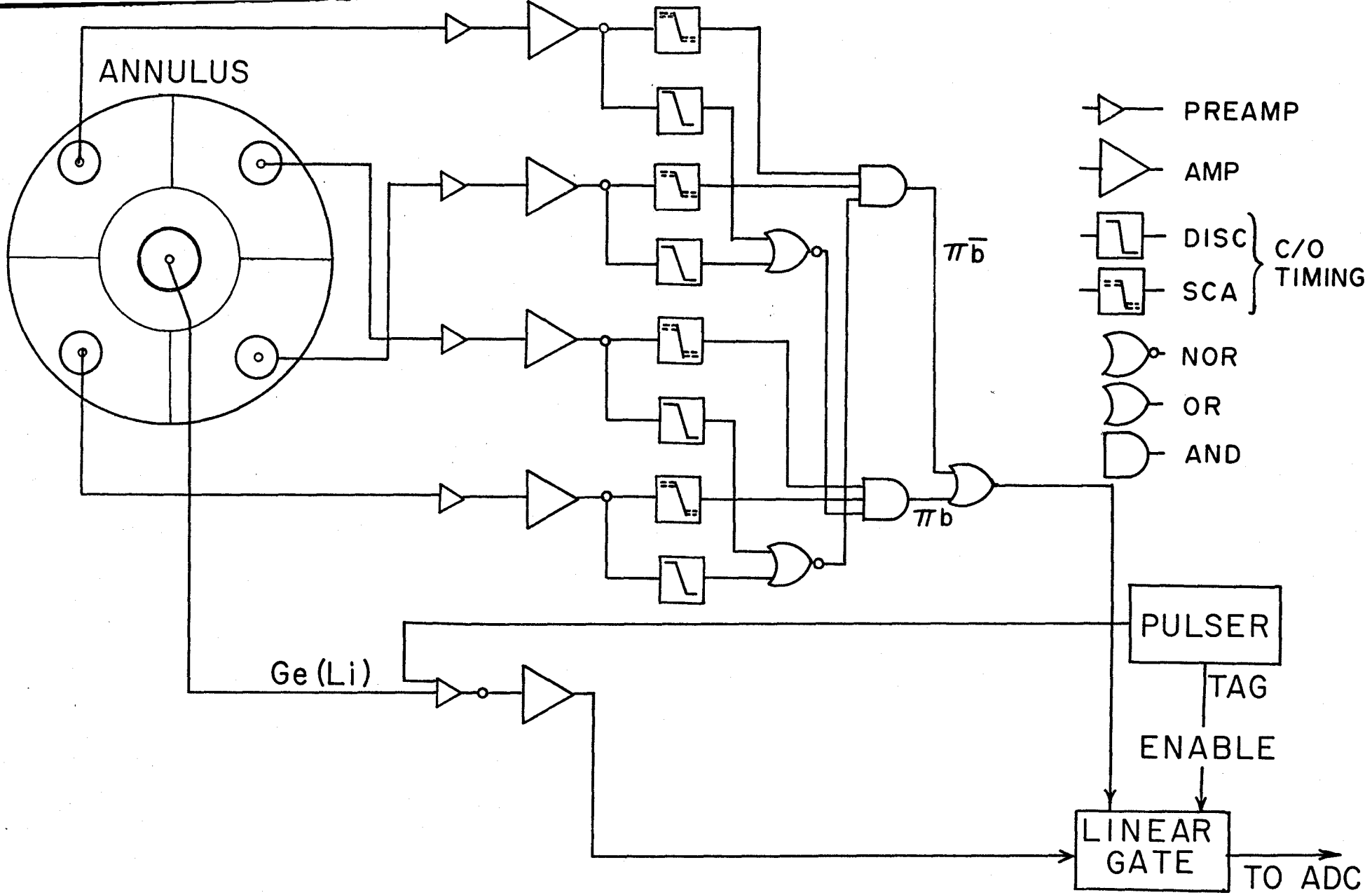

FIG. 2. CIRCUIT DIAGRAM

In Fig. (2), the schematic representation of the electronic configuration along with the Ge(Li) detector and NaI(Tℓ) quadrants is given. The central Ge(Li) detector has an active volume of 15 cm^3 and was fabricated by Princeton Gamma-Tech Inc. Surrounding it there is the quadrisected NaI(Tℓ) annulus, 15.2 cm long with inner and outer diameters of 8.6 and 23.0 cm (manufactured by the Harshaw Chemical Company). A photomultiplier tube is coupled to each quadrant and the signal is amplified in the usual manner. The purpose of the electronic components are self-evident from the diagram. The formation of the pair and bremsstrahlung conditions is a matter of straightforward logic circuitry.

The analogue pulses from the pair-spectrometer were digitized by a 50 MHz ADC and accumulated in an 8000 channel analyzer based on a Nova minicomputer. The pulser served as a reference for gain stabilization of the ADC.

CHAPTER 3

EXPERIMENT

3.1 THEORY

Let a sample of volume V contain n atoms of an element of interest which are distributed according to $n(\bar{r})$. The prompt gamma ray being detected occurs in a fraction, I, of neutron captures, and is detected with efficiency ε. Then, neglecting self absorption, events at this particular energy will be detected at a rate given by

$$R = I\varepsilon\int_V\int_0^\infty \phi(E,\bar{r})\sigma(E)n(\bar{r})dEd^3\bar{r} \qquad (3.1)$$

where $\phi(E,\bar{r})$ is the neutron flux density and assuming it is separable in position and energy (i.e. $\phi(E,\bar{r}) = \phi'(E)\phi''(r)$) this equation can be written as

$$R = I\varepsilon\int_V \phi'(\bar{r})n(\bar{r})d^3\bar{r}\int_V^\infty \phi''(E)\sigma(E)dE \ . \qquad (3.2)$$

Further assuming that almost all neutrons are thermal and the element is homogeneously distributed throughout the sample,

$$R = I\varepsilon\,\frac{n}{V}\phi''\sigma\int_V \phi'(\bar{r})d^3\bar{r} \qquad (3.3)$$

For a given sample with n_i atoms of nuclide i, the observed intensity of the γ-rays of energy E_j is

$$R_{ij} = I_{ij}\varepsilon(E_j)\frac{n_i}{V}\,\phi''\sigma_i\int_V \phi'(\bar{r})d^3\bar{r} \qquad (3.4)$$

In practice, $\phi(E,\bar{r})$, $\sigma(E)$ and ε are rarely known with sufficient accuracy. We considered the measurement of a known standard of sulphur (i=1) and silicon (i=2) with γ-rays j=a,b respectively. Eqn. (3.4) then leads to

$$R_{1a} = n_S\frac{1}{V}\,[I_{1a}\varepsilon(E_a)\phi''\sigma_1\int \phi'(\bar{r})d^3\bar{r}]$$

$$R_{2b} = n_{Si}\frac{1}{V}\,[I_{2b}\varepsilon(E_b)\phi''\sigma_2\int \phi(\bar{r})d^3\bar{r}]\ ;$$

(where n_S and n_{Si} are the number of atoms of the nuclides ^{32}S and ^{28}Si)

whence

$$(r_{12})_{stand.} = \left(\frac{R_{1a}}{R_{2b}}\right)_{stand.} = \left(\frac{n_S}{n_{Si}}\right)_{stand.} .k\ , \qquad (3.5)$$

where

$$k = \frac{I_{1a}\sigma_1\varepsilon(E_a)}{I_{2b}\sigma_2\varepsilon(E_b)}$$

k depends on the properties of the reaction and the

detector. For the unknown,

$$(r_{12})_{unknown} = \left(\frac{R_{1a}}{R_{2b}}\right)_{unknown} = \left(\frac{n_S}{n_{Si}}\right)_u .k \quad . \qquad (3.6)$$

From (3.5) and (3.6)

$$\left(\frac{n_S}{n_{Si}}\right)_u = \frac{1}{k} (r_{12})_u$$

$$= (r_{12})_u \cdot (r_{12})^{-1}_{stand.} \left(\frac{n_S}{n_{Si}}\right)_{stand.}$$

$$= (r_{12})_u \, \alpha_{S,Si}$$

where $\alpha_{S,Si} = (r_{12})^{-1}_{stand.} \left(\frac{n_S}{n_{Si}}\right)_{stand.}$ may be called the calibration constant.

Calibration samples were prepared to produce known values of $(n_S/n_{Si})_{stand.}$ and the corresponding $(r_{12})_{stand.}$ was determined by spectral measurement. Thus knowing $\alpha_{S,Si}$ from the calibration sample and $(r_{12})_u$ by spectral measurement of the unknown, $(n_S/n_{Si})_u$ can be determined from the formula

$$\left(\frac{n_S}{n_{Si}}\right)_u = (r_{12})_u \, \alpha_{S,Si} \qquad (3.7)$$

Similar calibration constants $\alpha_{Fe,Si}$ and $\alpha_{S,Fe}$ can be determined for (Fe,Si) and (S,Fe). They can be obviously used to determine the unknown n_{Fe}/n_{Si} and n_S/n_{Fe} ratios respectively.

(Here again, n_{Fe} is the number of atoms of the nuclide ^{56}Fe).

The quantity α should be a constant of the system so long as nothing interferes with the γ-ray peaks measured, and so long as there are no changes in efficiency function $\varepsilon(E_j)$. The first was checked by making standards from different compounds and different weight ratios. The second was a matter of stability and can be checked by measuring a specific standard immediately before and after the unknown.

It should be noted that n_S/n_{Si} and n_{Fe}/n_{Si} are actually the ratios of the nuclides of the elements. However, as the isotopic variations in each of these elements are not likely to be drastic in the samples, the nuclidic ratios may be supposed to be equal to the elemental ratios. Throughout the first part of this work the term 'elemental ratios' will be always used in place of 'nuclidic ratio'.

3.2 SPECIMENS OF MAIN SAMPLES

Allende Meteorite Sample :

The powdered specimen for irradiation was part of split number 4 (position 3) of a ground and homogenised sample prepared and distributed by the Smithsonian Institution, Washington D.C.

The bulk sample for irradiation was a chip from a specimen supplied by H.G. Thode.

Lunar Sample :

The chip for irradiation was a fragment from the sample 70215,80 supplied to H.G. Thode by the Lunar Receiving Laboratory.

70215 is a fine grained mare basalt from the Apollo 17 site.

3.3 PROCEDURE

For the sake of calibration, the mixtures of weighed amount of compounds given in table (1) were prepared in the laboratory. Each of the samples was ground for about an hour to make sure that the samples were homogeneous in their constituents, and thus to insure the identical irradiation condition for each constituent element of the sample. This procedure also insures that the correct

elemental ratio is preserved without the necessity for quantitative transfer to the irradiation capsule. Once the samples were in, the capsules were always kept roughly vertical with the bottom down so that the sample rested entirely in the bottom and gives maximum radiation through the tangential tube, while inside the core. Before finally putting the capsule in the core, the outside surface of the capsule was ground with cleaning paper lest it should have been contaminated by any previous handling.

TABLE 1

DATA FOR CALIBRATION SAMPLES

Sample	n_S/n_{Si}	n_{Fe}/n_{Si}	Hour of run	Capsule used as container
$CaSO_4+SiO_2$	.09048		73	C
$BaSO_4+SiO_2$	.11754		46	C
$BaSO_4+SiO_2$	.2289		50	C
$CaSO_4+SiO_2$	.08768		44	C
$CaSO_4+SiO_2$	.08768		60	C
$S + SiO_2$	.10248		67	C
$SiO_2+Fe_3O_4$		.3364	90	C
$SiO_2+Fe_3O_4$		.4931	70	C
$SiO_2+Fe_2(SO_4)_3$		.2591	88	C
$SiO_2+Fe_2(SO_4)_3$		.2591	60	C
$SiO_2+Fe_2(SO_4)_3$		.2768	69	Be

All calibration samples were contained in the graphite capsules excepting one which was contained in the beryllium capsule. Each of them were roughly 1 gm.

About .9 gm of homogenized powder of Allende meteorite **were** used in a beryllium capsule, previously thoroughly cleaned with methyl alcohol on an ultrasonic vibrator, and run on two different occasions. The same process was used for the lunar sample. In table (2), the facts regarding the run of these main samples are given.

TABLE 2

DATA FOR MAIN SAMPLES

Sample	Mass in gm	Physical Form	Hour of Run	Capsule used as container
Allende Meteorite	.9	homo. powder	140	Be
" "	"	" "	50	"
Lunar Sample	1	chunk	210	"
" "	"	"	260	"

3.3.1 INTERFERENCE

The presence of a wide variety of elements in Allende meteorite and moon rock makes it possible that there may be some other gamma rays interfering with the peaks we are considering for our analysis, namely, S(5420.5 keV), Si(3539.3 keV) and Fe(7632,7646 keV) (16). The potentiality of this interference is probed in tables (3) and (4). In these tables, interfering γ rays are arranged in increasing order of their distances from the centroid of the above peaks. The full width at half maximum of the peaks is 7.6 keV. For the determination of the peak areas, a region corresponding to 5 half widths was used. A peak will be said to be interfering with the main peak if the distance between their centroids is less than 5 half widths. With this definition, there can be two types of interference. In one case, the interfering peak is almost coincident with the main peak, while in the other, the peaks are resolvable by graphical or numerical analysis. In table (4), the interference of the peaks of P, Mg, Ti and Mn are of the second category. Using the intensity given in Ref. (16), iron seems to give a potentially interfering line with silicon. However

in the actual spectrum of a natural iron run of appreciably long time, we did not find any peak at all at that energy. In table (3) again, the interferences of P, Mn and Ni are easily amendable by graphical analysis or by computer programme. The only remaining significant and serious interference in sulphur is that due to iron. We took special care to correct for iron which would otherwise alter the S/Si ratio. Though the tables are shown for Allende Meteorite alone, it is to be noted that for the moon the only interference that deserves correction is the same as that for the meteorite. Since the sulphur content is particularly low in the moon rock, this interference is of great concern.

All other interferences in the three tables are negligible considering the accuracy involved in our final calculations.

The container capsules themselves may contain S, Si, or Fe. In fact the graphite or the beryllium capsule contains minute amounts of sulphur or silicon. Hence, it was necessary for us to run empty graphite and beryllium capsules for sulphur and silicon corrections respectively. Although these capsules contain some iron as well, the

amount of iron is too low to affect our results.

TABLE 3

POSSIBLE INTERFERENCE
WITH S 5420.2 keV PEAK

Element	Atomic weight	*Energy level in keV	*Intensity No/100	$\sigma\gamma$ in barns	Elemental abundance in Allende in ppm unless otherwise indicated	Relative yield normalised to Silicon or iron
S	32.064	5420.5	60	.52	2.1%	100
Fe	55.847	5420.6	.04	2.55	23.6%	2.12
P	30.974	5422.7	.24	1.9	.11%	0.08
Cu	63.546	5417.7	2.02	3.8	130	0.10
Sr	87.62	5424.1	.9	1.4	14	0.001
Aℓ	26.981	5411.1	1.11	.234	1.74%	0.16
Mn	54.938	5435.7	2.09	13.3	.15%	3.70
Ni	58.71	5436.0	.55	4.57	1.42%	2.93

POSSIBLE INTERFERENCE
WITH Fe (7632-7646 keV)
DOUBLET

Fe	55.847	7640.0	49.33	2.55	23.6%	100
Cu	63.546	7635.6	14.47	3.8	130	.02
Sc	44.956	7635.9	2.58	25	11	.004

* For S, these values are taken from Ref. (4 to 6) and for all other elements, from (16).

TABLE 4

POSSIBLE INTERFERENCE
WITH Si 3539.3 keV PEAK

Element	Atomic weight	*Energy level in keV	*Intensity No/100	σγ in barn	Elemental abundance in Allende in ppm unless otherwise indicated	Relative yield normalised to Silicon
Si	28.086	3539.3	79.58	.16	16%	100
Fe	55.847	3540.1	.1	2.55	23.6%	1.4
Zn	65.37	3535.9	.18	1.10	120	.0005
V	50.942	3534.5	.59	5.03	90	.007
Na	22.9898	3546.0	6.7	.98	.34%	.0001
K	39.102	3546.6	4.26	2.1	250	.079
Cℓ	35.453	3531.7	.11	33.3	220	.031
N	14.0067	3530.5	9.58	.08	62	.0047
Aℓ	26.9815	3530.3	.16	.234	1.74%	.033
Mg	24.305	3549.6	.34	.063	14.9%	.18
Ti	47.90	3554.2	1.41	6.1	900	.220
Mn	54.938	3555.5	.28	13.3	.15%	.138
P	30.9738	3522.8	14.49	.19	.11%	.135
F	18.9984	3522.3	12.13	.01	59	.0005
Sc	44.956	3556.3	.27	25	11	.002

* Ref. (16)

To determine the contribution from the graphite capsule to the sulphur in our sample, a representative empty graphite capsule was run for 114 hours. Similarly for figuring the silicon contribution by the Be capsule, an empty capsule was run for 50 hours.

Natural iron was run in order to determine the ratio between the area of the 5.42 MeV peak and that of the 7632-7645 doublet and thus to assess its contribution to the sulphur peak in the spectra in which both iron and sulphur were present. Table (5) gives the experimental conditions for measurements involving natural iron compounds.

TABLE 5

DATA FOR NATURAL IRON

Sample	Mass of the compound in gm	Counting Period	Capsule used as container
Fe_3O_4	.4	44	C
Fe_2O_3	.6	65	Be
Fe_2O_3	.5	96	C

CHAPTER 4

DATA ANALYSIS

The selection of gamma transitions for the analysis was based on two considerations. The lines should have high intensity and they should be comparatively free from interference.

The elements of major interest are silicon, sulphur and iron. In order to make corrections for interference, we are also concerned with beryllium and carbon. The suitable lines for their analyses are Be(2589.9) and C(3683.9). Another peak of iron to be considered is Fe(5420.6), the one which is coincident with the sulphur peak.

For the determination of the peak area a certain energy window for each peak was chosen. Proper care was taken so that the same peak in all different spectra had the same energy window around its centroid.

Before going into the specific discussion of the analysis, let us at this point briefly describe rather qualitatively what was done. Consider the problem of the determination of the n_S/n_{Si} ratio in the Allende

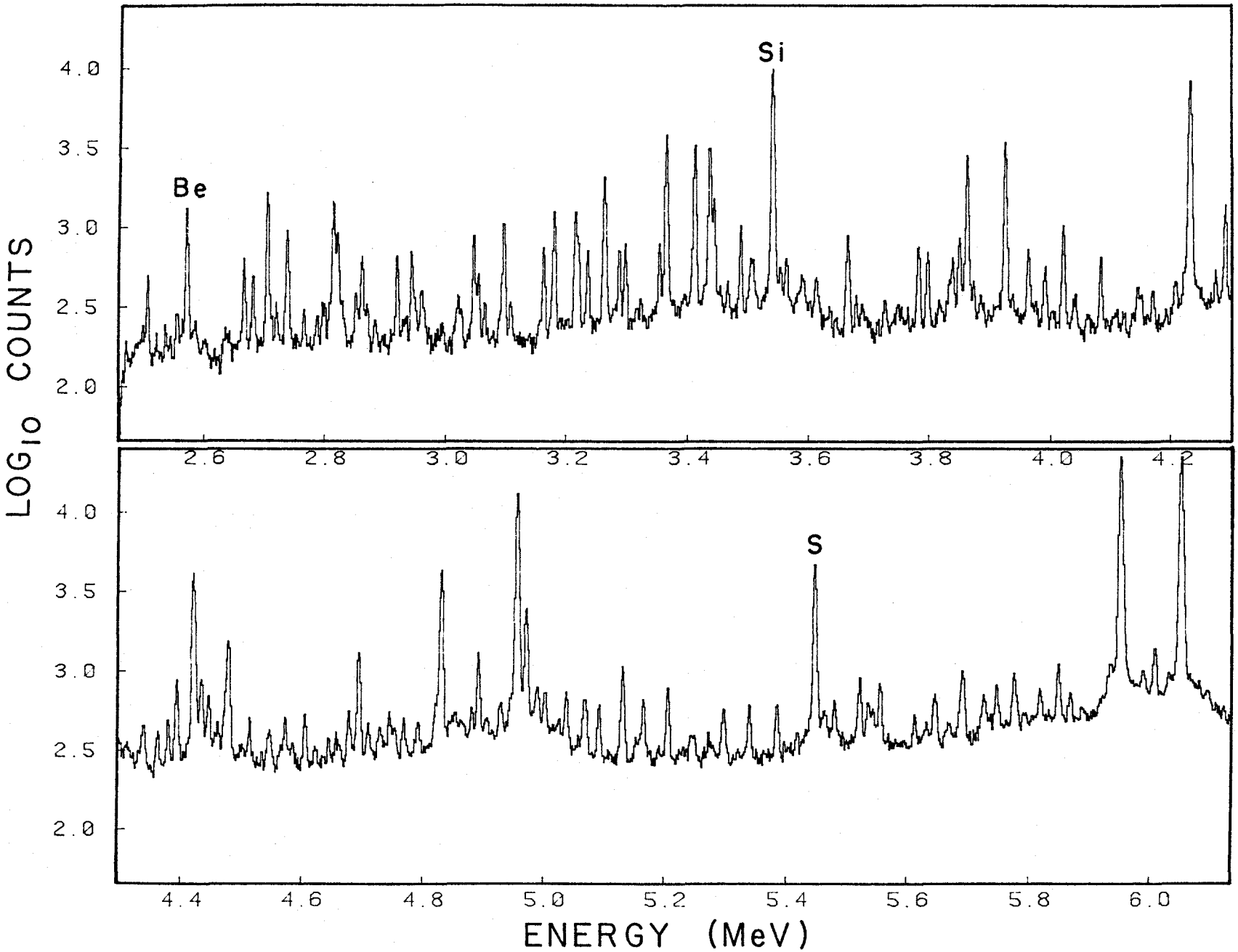

Fig. 3 Spectrum of the Allende meteorite sample.

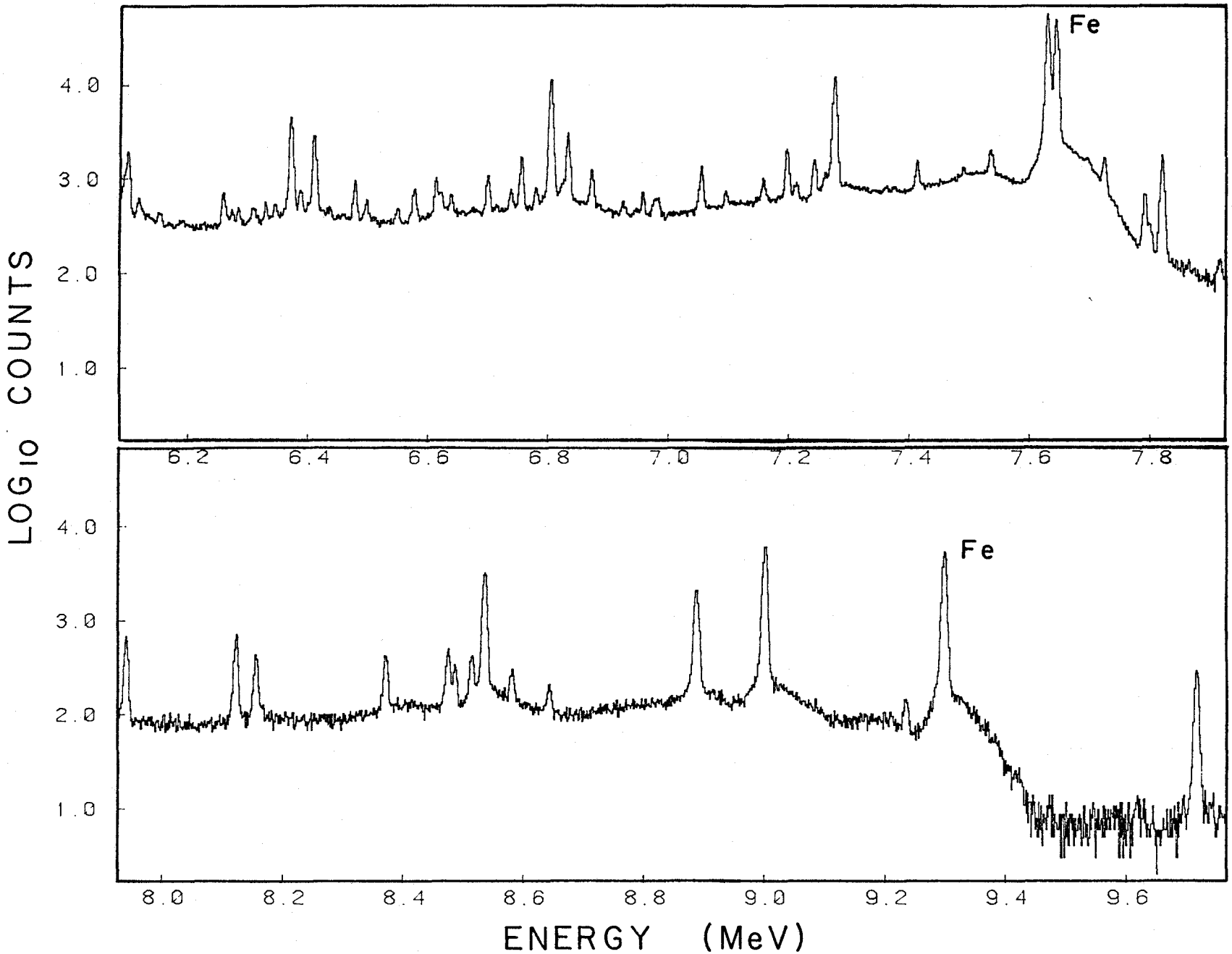

Fig. 4 Spectrum of the Allende meteorite sample.

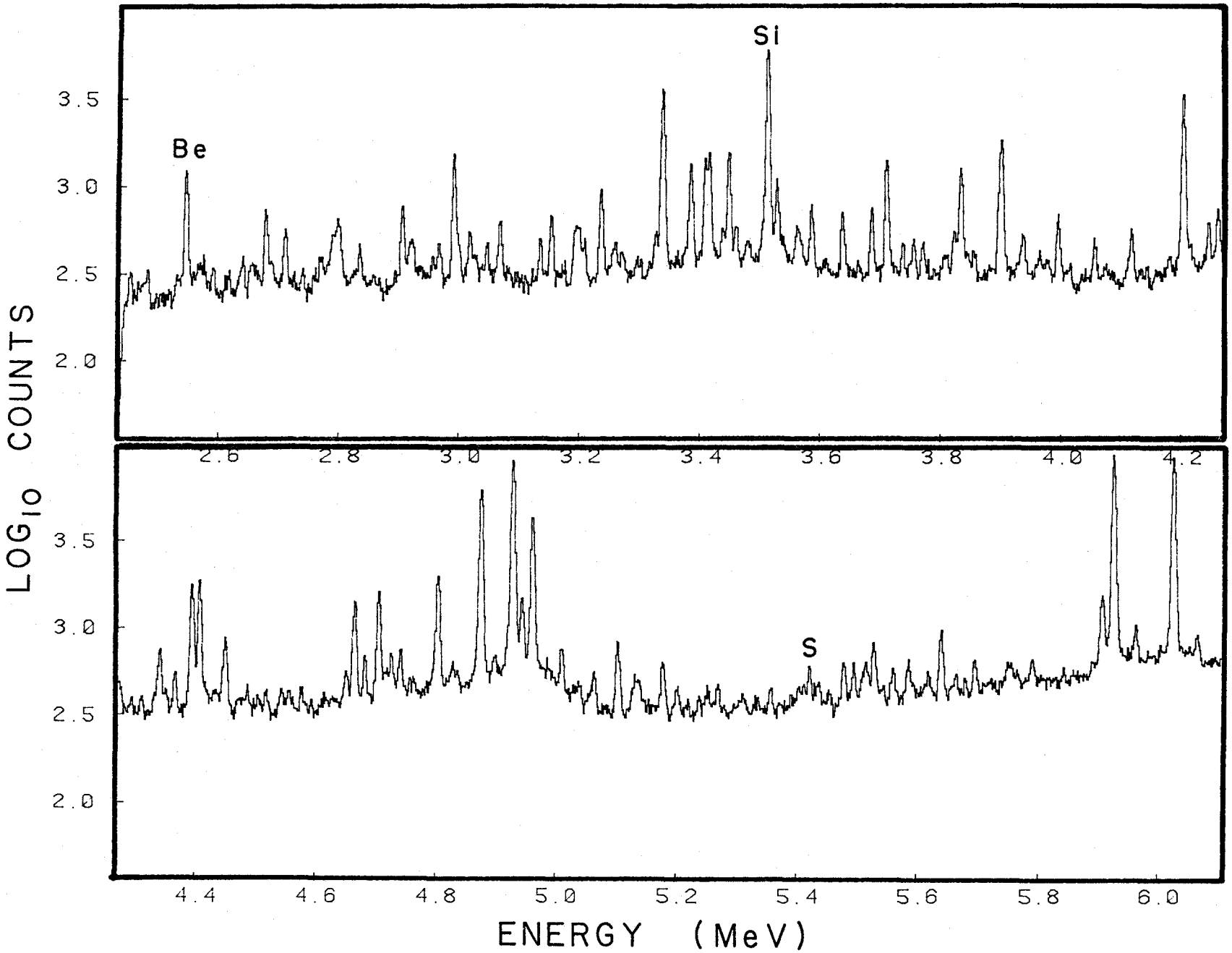

Fig. 5 Spectrum of the lunar sample.

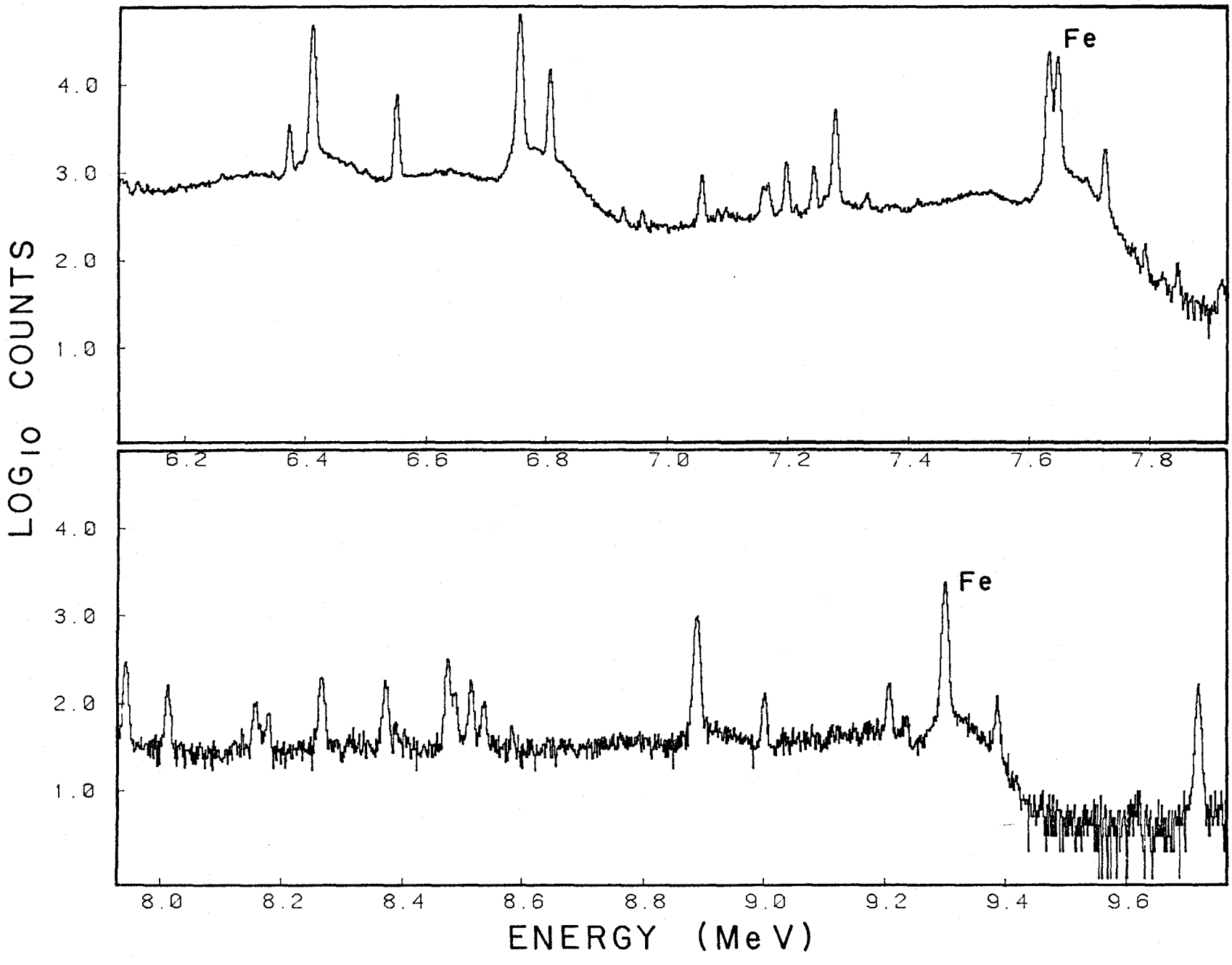

Fig. 6 Spectrum of the lunar sample.

meteorite. From the spectrum of the calibration sample the areas of the sulphur and silicon peaks were determined. But the calibration sample was contained in a graphite capsule which itself contained small amounts of sulphur. In the spectrum of the empty graphite capsule run, the ratio between the areas of the C peak and S peak was determined. Multiplication of this ratio with the area of the C peak in the calibration sample gave the sulphur contribution from the graphite capsule. The ratio of the corrected area of the sulphur to silicon peak, divided by the known n_S/n_{Si} gave the calibration constant $\alpha_{S,Si}$. Then from the spectrum of the Allende meteorite the areas of the sulphur and silicon peak were determined. The latter was corrected for the contribution from Si in the Be capsule. Correction of the sulphur peak area for Fe interference in the Allende spectrum was essential as the Allende sample contains a significant amount of iron. From the natural iron run the ratio of the areas of the 5420.6 peak to that of the 7460 keV doublet was calculated. This constant along with the area of the iron doublet in the Allende spectrum, gave the correction

for the sulphur peak. The ratio between the corrected silicon and sulphur peak area while multiplied with the calibration constant gave the n_S/n_{Si} in Allende.

It is obvious now that if in the calibration sample any iron compound was used, the sulphur peak area should be corrected for the iron peak contribution as was done in the case of Allende.

To find the net area of a peak, the background area was subtracted from the gross area. A definite region about the centroid was selected for integration to obtain the gross area. The contribution from the continuum was estimated from adjacent regions assuming a linear variation. Symbolically,

$$S = \sum_{i=i_1}^{i_2} Si - \sum_{j=j_1-(i_2-i_1+1)/2}^{i_1-1} Sj - \sum_{k=i_2+1}^{i_2+(i_2-i_1+1)/2} Sk \qquad (4.1)$$

where Si constitutes the gross area and Sj and Sk, the continuum and the subscripts refer to the channel numbers.

In a few cases some smaller peaks overlapped with the main peak or interfered with the background of the latter. The peaks were then resolved graphically and

the area of the resolved peaks were determined from the graph in the same way stated above.

4.1 IRON CORRECTION

Two independent measurements of natural iron in the form of Fe_2O_3 were performed. In the first the sample was contained in a beryllium capsule and there was no interference with the doublet and Fe(5420.6) peak. The ratio of the peak areas was determined to be .00072 ± .00015 In the second case, the sample was in a graphite capsule and a correction was necessary for the contribution from sulphur in the capsule material to the area of Fe(5420.6) peak. The correction was 20%. The ratio obtained was .0008 ± .0001. The weighted average of the two values is .00076 ± .00009.

4.2 Be AND C CAPSULE CORRECTION

In the beryllium capsule spectrum the ratio of the areas of the Si(3539.3) and Be(2589.9) peaks was found to be .062 ± .012. The ratio of S(4520.5) to C(3683.9) as determined from the empty graphite capsule run was .0077 ± .0030.

4.3 CALIBRATION SAMPLE ANALYSIS

There are 11 independent runs of various calibration samples mentioned in section (3.3). Nine of them were utilized for checking the dependence of the calibration constant on the compound or the weight ratios. It was found to be independent of the compound or the weight ratios.

For the actual measurement, calibration was performed at the time of run of the unknown.

4.4 DATA ANALYSIS FOR ALLENDE METEORITE

There were two independent measurements of the spectrum of the Allende meteorite. The data was analysed graphically.

The iron contribution to the 5420 keV peak for both runs was about 2%. The Be-capsule correction was .7%. The values obtained were

$$\frac{n_S}{n_{Si}} = .116 \pm .002$$

for the first run, and

$$\frac{n_S}{n_{Si}} = .117 \pm .003$$

and

$$\frac{n_{Fe}}{n_{Si}} = .735 \pm .012 \text{ for the second run.}$$

4.5 DATA ANALYSIS FOR LUNAR SAMPLE

The determination of n_S/n_{Si} in the lunar sample faced certain difficulties. As seen in Fig. (7), there are several peaks in the sulphur region interfering with both the background and the main peak.

We had two independent runs of the same lunar sample and thus two spectra for analysis. From each of these spectra, a suitable section of 81 data points indicated in the figure was analysed by the method of least squares. The data were fit to a model consisting of a constant background and 10 Gaussian peaks for the first spectrum, and 9 Gaussians for the second. The extreme left small peak used in the first spectrum could not, in any way, be fit in the second. The reason for this is not understood. However, the subsequent net area of the sulphur peak was almost insensitive to this alteration.

The area of a fitted Gaussian peak is in general less than the actual peak area by a value depending on the chi square (17). In addition, this area is sensitive

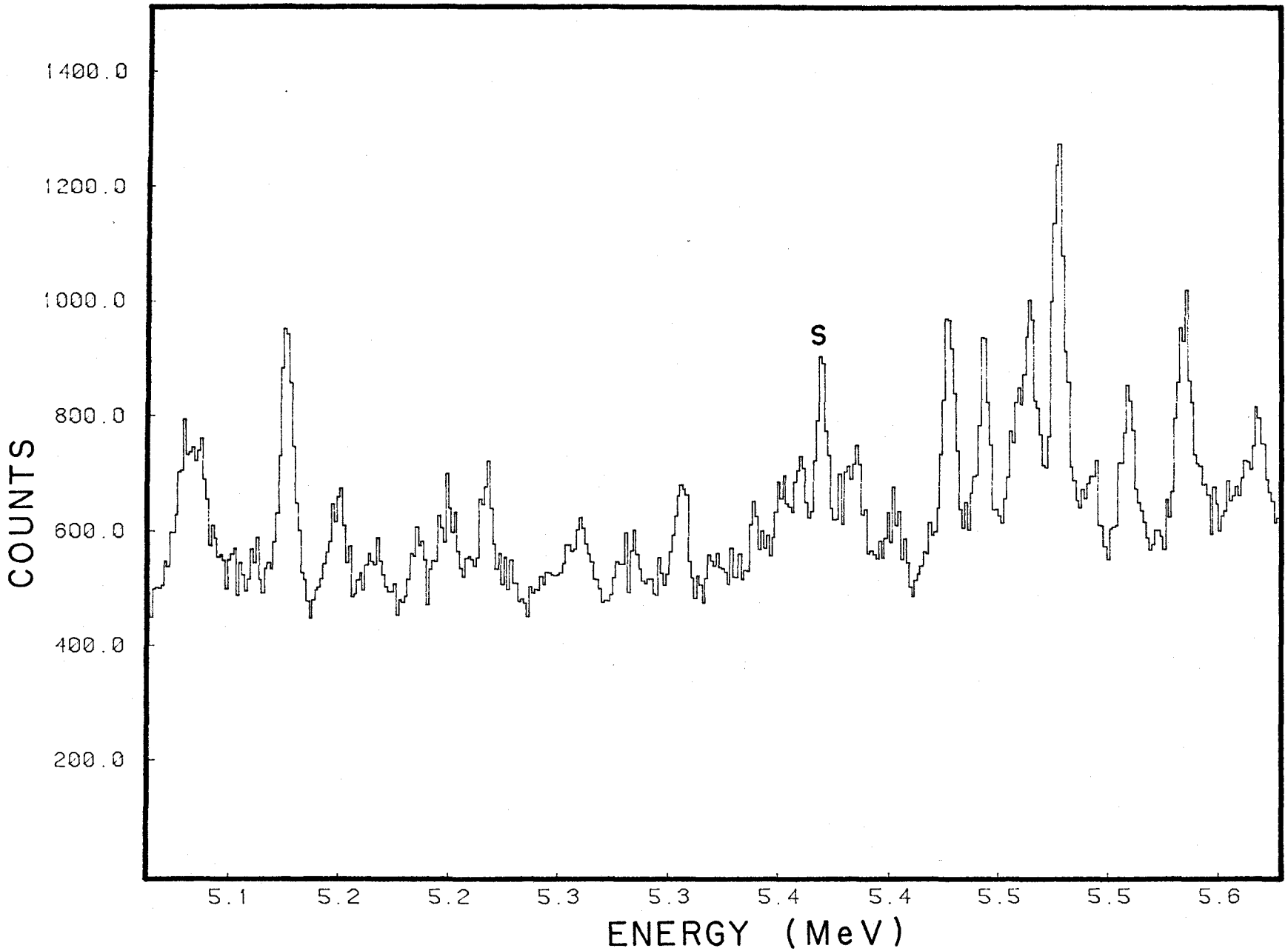

Fig. 7 Sulphur region of the lunar sample spectrum.

to the shape assumed for the peak. Therefore an alternative approach for determining the net area was adopted. The spectrum in the region resulting from the contribution of the interfering components was reconstructed from the model. This spectrum was then subtracted from the original data. The residual spectrum thus corresponds to the contribution from the sulphur-iron complex. The positions of the centroids were suitably varied to minimize chi square and thus the best fit was obtained. The width of the peaks was determined from the FWHM of a more intense single peak at a distance of 220 keV from the sulphur peak in the original spectrum. The FWHM values were 5.27 and 6.12 channels respectively. In each case a slight variation around these values did not appreciably alter the sulphur peak area considering the error involved in the latter value. Moreover corresponding to these values the chi square was minimum. In Fig. (8) the data points, the fitted curves and the residual sulphur peak are displayed. Fig. (9) shows the variation of the chi square with the background in the first spectrum. The variance in the net area of the sulphur peak was determined by the formula:

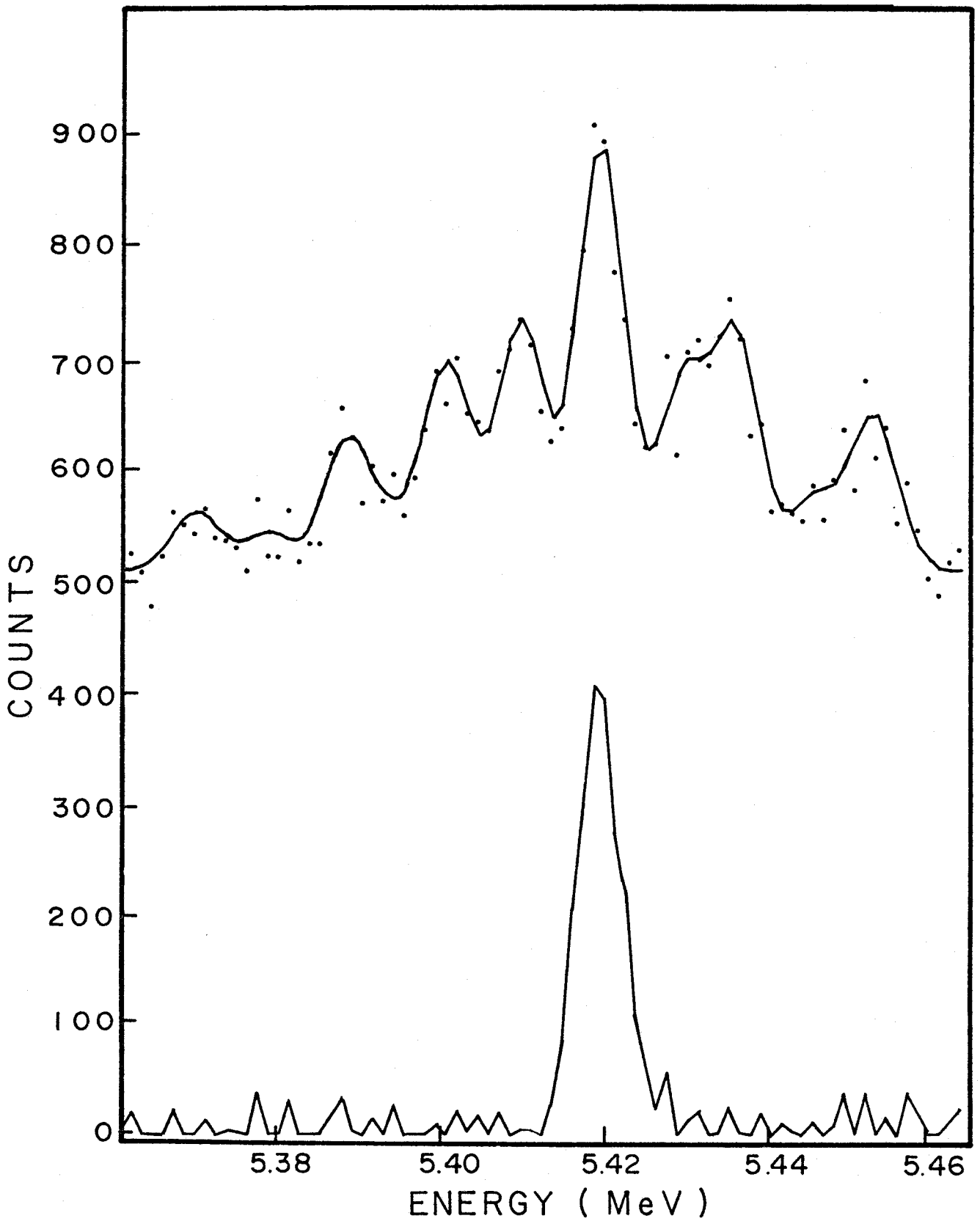

Fig. 8 (a) The smooth curve is the least square fit of the sulphur region of the lunar sample with Gaussian model; (b) Residual spectrum after substracting the fitted spectrum of the non-sulphur components.

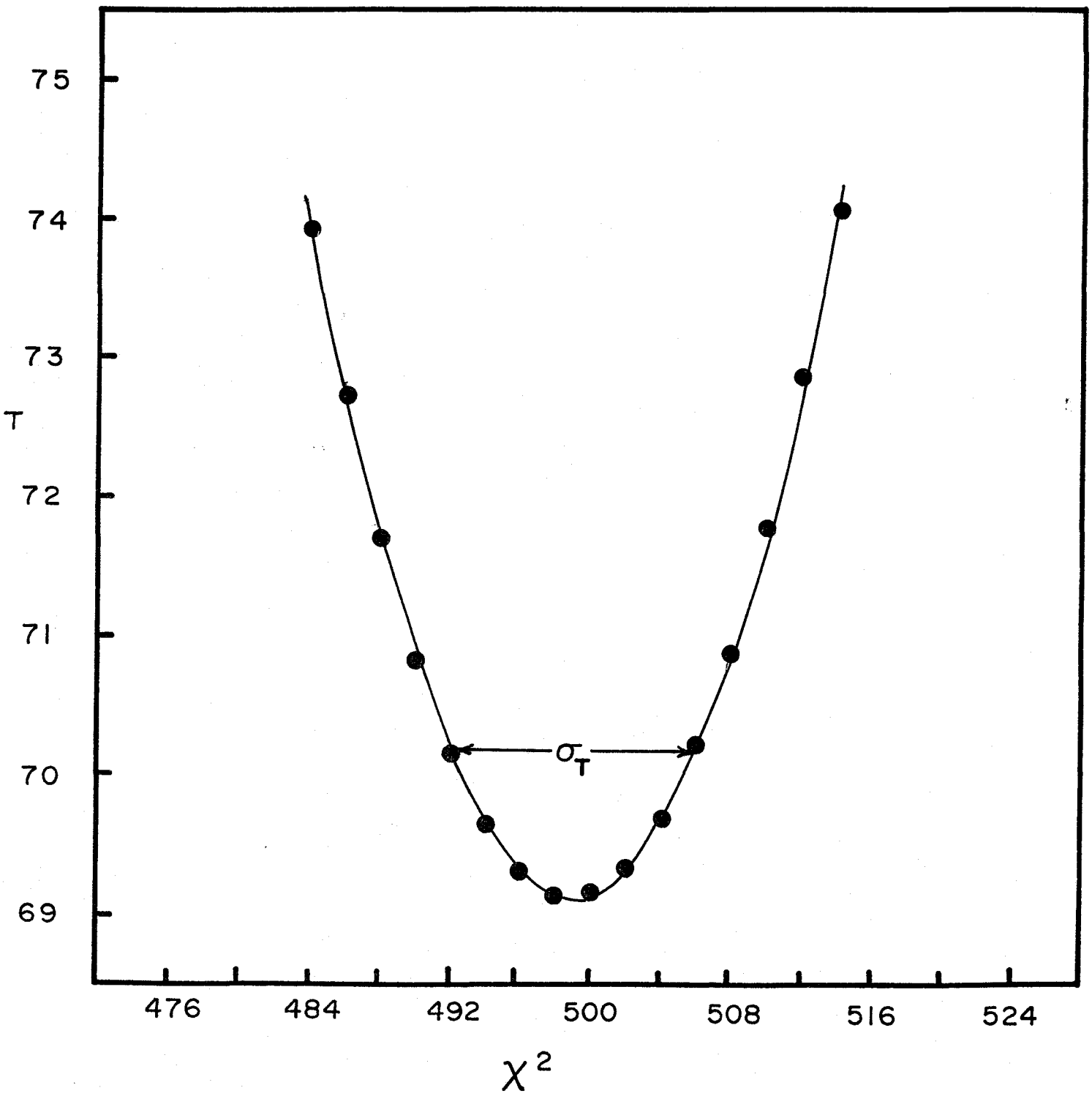

FIG.9 VARIATION OF CHI SQUARE WITH BACKGROUND

$$\sigma^2 = N_{gross} + K^2\sigma_T^2 \frac{\chi^2}{f}$$

$$N_{gross} = N_{net} + KT$$

where f is the number of degrees of freedom. In the two analyses, f = 69 and 68 respectively, K is the channel window for the sulphur peak. The standard deviation in T, σ_T, as shown in Fig. (9) is double the change in background for which the change in χ^2 is 1. Its value for the first and the second, are 13.5 and 15 respectively. The reduced chi squares in the measurements were 1.002 and .917 respectively.

Once the area of the sulphur-iron complex was obtained, the correction for the iron peak contribution at the sulphur peak was made. To appreciate the error and the percentage correction involved table (6) can be noted.

TABLE 6

IRON CORRECTION FOR SULPHUR

Identity of the spectrum	Area of sulphur-iron complex	Area of iron peak	Correction involved %	Area of sulphur peak
1	2249±230	362±45	16	1887±303
2	2304±209	331±42	14	1973±267

The ratios sulphur/silicon obtained are

$$\frac{n_S}{n_{Si}} = .0084 \pm .0011 \quad \text{and}$$

$$\frac{n_S}{n_{Si}} = .0088 \pm .0012$$

in the first and second run respectively. Taking their average, converting them to mass ratio and using the known value (29) of percentage of Si in the lunar sample, the sulphur content was found to be (1730 ± 180) ppm.

In the similar way, knowing the area of the iron doublet in the second run (we did not run a calibration sample of iron for the first run) we obtained

$$\frac{n_{Fe}}{n_{Si}} = .444 \pm .005$$

as the ratio of number of atoms of iron to silicon.

CHAPTER 5

DISCUSSIONS OF RESULTS

The elemental ratios S/Si and Fe/Si in the bulk Allende meteorite and in the lunar sample as obtained by this work are presented in tables (7), (8), (9) and (10) respectively along with several values reported by other groups by various methods.

TABLE 7

S/Si RATIO IN ALLENDE METEORITE

Bulk		*Matrix		*Chondrules	
n_S/n_{Si}	Ref.	n_S/n_{Si}	Ref.	n_S/n_{Si}	Ref.
.1734	[18]	.0753	[21]	.0432	[18]
. 113	[18]	.1358	[18]		
. 115	[19]				
.0924± .0024	[20]				
. 116± . 002	This work				

* For the definitions of the terms see section (6.4).

TABLE 8

Fe/Si RATIO IN ALLENDE METEORITE

Bulk		Matrix	
n_{Fe}/n_{Si}	Ref.	n_{Fe}/n_{Si}	Ref.
.7503	[18]	.9515	[21]
.7403	[22]	.8630	[18]
. 742	[19]		
. 861	[23]		
. 725	[23]		
. 742 ± . 008	[20]		
. 735 ± . 011	This work		

The value of n_S/n_{Si} in the bulk Allende agrees well with those of Clarke et al. (18) and B. Mason (19). The same ratio in the matrix should be higher as is reported by Clarke et al. because it is much lower in the chondrules (18). The lower value (Harry et al.) of the ratio in the matrix, on this ground, does not seem to be tenable. One of the values of n_S/n_{Si} in the bulk

exceeds that in the matrix and thus is not acceptable. The comparative low value obtained by the same method by W.V. Prestwich may be due to the fact that he used an inhomogeneous sample of Allende meteorite instead of the homogenized sample as used in this work. The former might happen to contain more chondrules than a representative sample does and thus might contain comparatively less sulphur.

The reported values of n_{Fe}/n_{Si} agree well among themselves and with the value obtained in this work. The only value drastically differing from the rest was reported by King et al. who determined the value by optical emission method and it throws doubt on the applicability of this method to this particular problem.

The NCGA method is thus found to produce reasonably acceptable values of these two elemental ratios in the bulk Allende meteorite.

TABLE 9

S/Si RATIO IN LUNAR SAMPLE

Sulphur content in ppm	$*n_S/n_{Si}$	Ref.
1581	.00783	[1]
1600	.00793	[1]
1630	.00808	[1]
1689	.00837	[24]
2040	.01011	[25]
2210	.01095	[26]
1730±200	.0086±.0010	This work

* All but the last value of this column are obtained by dividing the sulphur content reported in the literature by well-known silicon content (29). The reverse way is followed in this work.

TABLE 10

Fe/Si RATIO IN LUNAR SAMPLE

n_{Fe}/n_{Si}	Ref.
.435	[27]
.441	[28]
.422	[29]
.444 ± .005	This work

Before this work several values of sulphur content in the Apollo 17 rock sample 70215 were reported. The values, as are apparent from table (9) distinctly fell into two groups : one, between ∿ 1600 to ∿ 1700 and the other, between ∿ 2000 and ∿ 2200. These values were determined by different chemical methods. In contrast, the method used in this work is an instrumental method, thereby avoiding possible difficulties due to dependence on chemical form. The values of this work do not support the second groupings. In fact, they overlap with values reported by C.E. Rees et al. As discussed previously, NCGA has determined the n_S/n_{Si} value for Allende meteorite, which agree well with other reported values. It is also noted in table (10) that n_{Fe}/n_{Si} determined in a similar way is in reasonably good agreement with other published values. The same method, therefore, is likely to correctly determine the n_S/n_{Si} for the lunar sample. The inherent problem in the lunar sample analysis gave rise to appreciable error. Nevertheless the values obtained agree within error with those of Rees et al. which were obtained by three different methods. Thus NCGA method has been successfully applied to this particular problem resolving the contradiction in the literature.

PART II

EVIDENCE FOR AN ISOTOPIC ANOMALY IN IRON FROM THE ALLENDE METEORITE

CHAPTER 6

INTRODUCTION

6.1 METEORITES

Meteors are extra-terrestrial bodies, ranging from very large ones weighing many tons to tiny particles of dust, which are heated to incandescence as they pass through the earth's atmosphere. The larger meteors may be seen at night as glowing particles streaking across the sky. Most of them are burnt up and vapourized completely during their trip through the atmosphere. The bodies which are not completely burnt up and destroyed during their flight but survive to reach the earth's surface, are called meteorites.

A meteorite may strike the ground as a single body, or be fragmented during its flight through the atmosphere and arrive at the earth's surface as a shower of small particles. During the atmospheric passage, meteorites may suffer severe material loss by ablation. The energy of impact with the earth sets an upper limit for the recovered masses of meteorites: for a mass greater than about a hundred tons the impact energy is

sufficient to vapourize the entire body. The so-called meteorite craters are the relics of such impacts where almost no traces of the original body have remained.

Up to the time of the lunar sampling expeditions meteorites were the only available extra-terrestrials and for many years have been the subject of investigation by workers in astronomy, astrophysics, chemistry, geology, geophysics and nuclear physics. Certain classes of meteorite probably represent matter in a primitive pre-planetary condition while lunar and terrestrial materials have undergone extensive periods of preplanetary and planetary evolution and alteration. Thus the meteorites present multifarious peculiarities unknown in terrestrial or lunar geology.

6.2 THE ALLENDE METEORITE

The Allende meteorite fell in northern Mexico in 1969 at a time when many laboratories were equipped for research on the lunar sample that would be brought by Apollo 11 expedition only a few months later.

The Allende is the largest recorded stony meteorite fall both in terms of the areal extent and the mass of

material collected. As discussed in the next section, it is a carbonaceous chondrite, a rare class of meteorite (only 30 in all, out of about 2000 known meteorites (19)) but one of special significance for cosmochemistry and astronomy. Recent studies show that the carbonaceous chondrites probably approximate samples of the condensable fraction of primordial solar-system matter. These meteorites, therefore, have been of great interest to researchers in the field of cosmochemistry. Before Allende the carbonaceous chondrites were few in number and the total recovered mass was small. The Allende meteorite contributed 2 tons of material giving scientists the ample opportunity to carry out their research by various methods for petrographic and mineralogic investigation, and isotopic and elemental analysis. It was, for the first time, possible to prepare a representative portion of a carbonaceous chondrite as a homogeneous powder and distribute it for analytical and other purposes.

6.3 CLASSIFICATION OF THE ALLENDE METEORITE

In order to appreciate the classification of the Allende meteorite it is necessary to review the classification of meteorites in general. Obviously, we shall

concentrate our discussion mainly around the particular class to which the Allende belongs.

6.3.1 CLASSIFICATION OF METEORITES

Meteorites are found to fall into three distinct classes:

(a) the irons, which are always associated with a certain amount of nickel;

(b) the stones, which are mainly silicates;

(c) the stony irons, which as the name implies, are a mixture of the previous two.

The greater proportion of the meteorites found on the earth's surface (finds) are irons while stones account for only one-quarter. However, among meteorites which are observed to fall (falls) there are 80% stones, but only 6.5% irons. The reason for this apparent difference is that the stony meteorites resemble certain terrestrial rocks, and because of their greater tendency to weather, they escape detection much more easily if they are not recovered soon after the fall. The blocks of nickel-iron, on the other hand, resist weathering and are generally so conspicuous that they can be easily recognized.

Irons consist of mainly iron and nickel abundances 95 to 85% and 5 to 15% respectively. In addition, cobalt, chromium, phosphorus, sulphur and carbon are present as minor or trace elements. The main constituents of the stony meteorites are oxygen, silicon, magnesium and iron in the form of magnesium-iron silicates with calcium, sulphur and aluminum in much smaller abundances. The general classification of meteorites is shown in Fig. (10). We are particularly interested in the chondrite branch of the stones.

Most of the meteorites which fall are chondrites, so named because they contain variable amounts of chondrules i.e. spheroidal or ellipsoidal bodies usually a few tenths of a millimeter to a few millimeters in diameter. The mineralogy of the chondrules is essentially the same as that of the matrix in which they are embedded. Chondrules often account for 70% or more of the mass of a given chondrite. Chondrule-like bodies are rare or absent in terrestrial rocks. Chondrule-containing meteorites are very similar to one another in their major and minor element contents with the exception of some highly volatile elements. The relative amounts of non-volatile

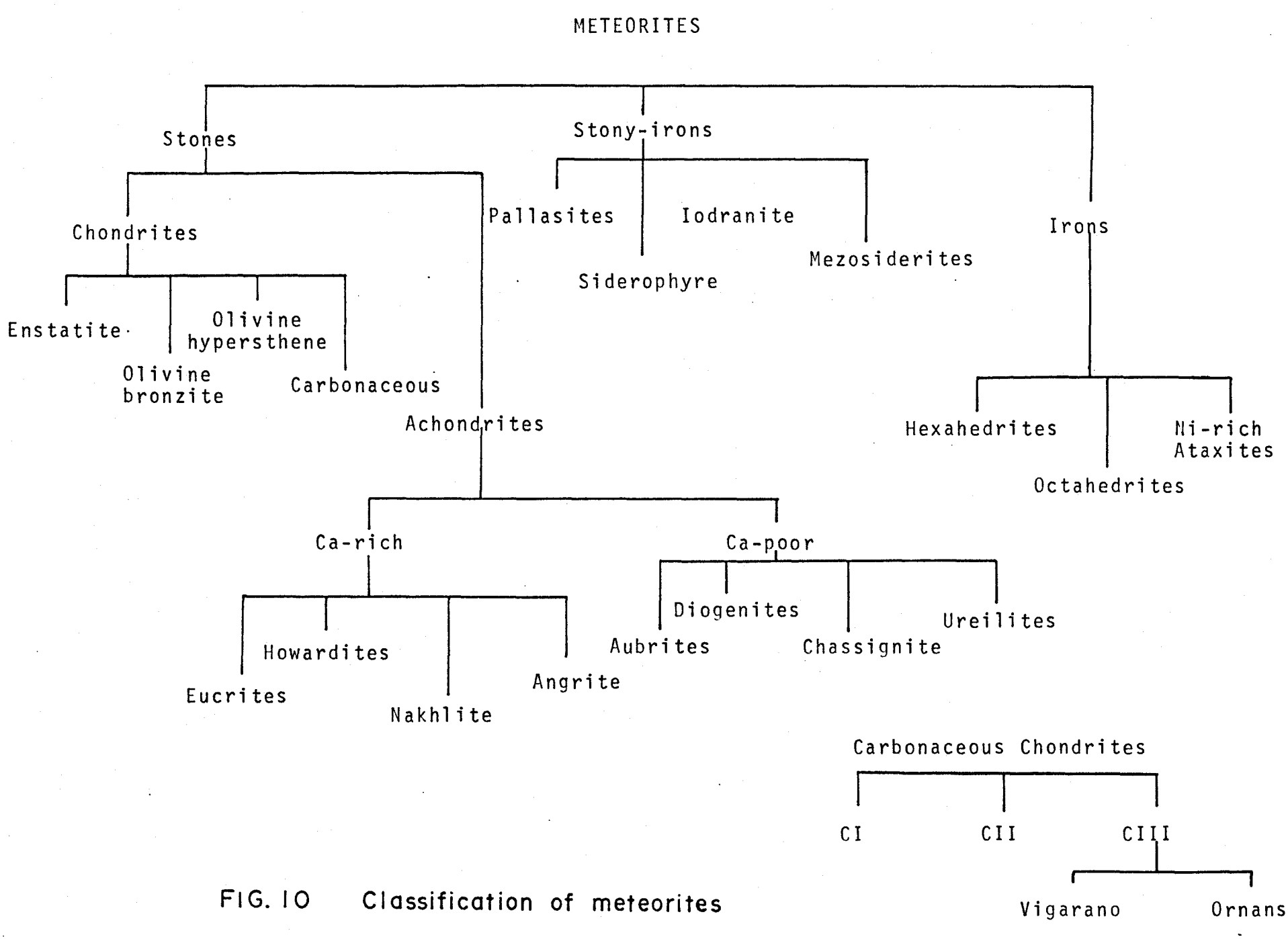

FIG. 10 Classification of meteorites

elements in chondrites are remarkably similar to those found in the atmosphere of the sun and stars similar to the sun. A number of other meteorites are known in which chondrules are absent, but in which the non- volatile elemental content is very similar to that of the chondrule-rich meteorites. Such meteorites are also called chondrites.

The chondrites were subgrouped in the following way by Van Schmus and Wood (31).

Enstatite: These meteorites have a higher total iron content (up to 35%) and a much higher SiO_2/MgO ratio than other chondrites. Principal minerals are enstatite ($MgSiO_3$) and iron-nickel ($(Fe,Ni),FeNi_3$).

Carbonaceous: Although the name implies a higher carbon content, this is not the main distinguishing factor. These meteorites contain organic compounds and hydrated minerals. The members of this group have lower SiO_2/MgO ratios than those of the groups described below, and are very deficient in metallic iron. Some do not contain chondrules, and the constituent minerals show great variations from one to another.

Bronzite: These meteorites have the highest Fe/SiO_2 ratios and also the highest metallic iron-to-total iron ratios reflecting their relatively lower degree of oxidation. The group is also known as H-chondrites (H for high iron content). Main minerals are olivine $(Mg,Fe)_2SiO_4$ and bronzite $Mg_{.70-.88}Fe_{.30-.12}\ SiO_3$. Total average iron content is 28% by weight.

Hypersthene: These meteorites are distinguishable from the H-chondrites by their lower total iron content (22%, by weight). Members of this group are also called L-chondrites (L for low iron content). The main minerals are olivine, hypersthene $Mg_{.5-.7}Fe_{.5-.3}SiO_3$ and nickel-iron.

Amphoterite: These meteorites, also called LL-chondrites, are similar to the hypersthene meteorites, differing from them only in total iron content (18% by weight).

Carbonaceous Chondrites: Although there are further subtypes according to petrologic properties within each type of the chondrites just described, we

shall limit detailed discussion to carbonaceous chondrites because it is to this group that the Allende meteorite belongs.

According to Wiik (30), carbonaceous chondrites can be divided into three types CI, CII, and CIII. This division is based on his numerous chemical analyses. Some of the principal distinguishing factors are C, H_2O, total S, and specific gravity, the mean values being:

	C(%)	H_2O(%)	S(%)	S.G.
Type I	3.54	20.08	6.04	2.2
Type II	2.46	13.35	3.16	2.7
Type III	0.46	0.99	2.21	3.4

These three types are clearly demarcated both by chemical and mineralogical criteria, and appear to be discrete groups, meteorites of intermediate composition being unknown. There is, however, one unique carbonaceous chondrite, Renazzo, which cannot be readily classified; its mineralogy resembles that of type II, except for the presence of 12% free nickel-iron.

Depending on the textural and other distinctions there are again two subtypes of the CIII chondrites,

provisionally called the Vigarano and the Ornans subtypes. The chondrites belonging to the Vigarano subtype may be characterized as having large (1-2 mm diameter) 'spongy' chondrules embedded in an abundant, fine-grained, opaque matrix; 'spongy' chondrules contain numerous spheroidal droplets of nickel-iron or sulphide dispersed throughout them. The chondrites belonging to the Ornans subtype may be characterized as a close-packed aggregate of small (0.2-0.5 mm diameter) metal-poor chondrules with fine-grained, opaque matrix packed between the chondrules. To be more specific, a number of criteria for distinguishing between these two subtypes are listed (32) in table (11).

TABLE 11

DISTINCTIONS BETWEEN VIGARANO AND ORNANS

	Chondrule size (mm)	Chondrule/ matrix ratio	Atomic Ratios Aℓ/Si	Ca/Si	Fe/Mg	Ar/ Xe	^{36}Ar ($10^{-8}cm^3gm$)
Vigarano subtype	0.5-2	∿ 0.5	$\geq$0.12	$\geq$0.08	$\leq$0.76	∿100	$\leq$30
Ornans subtype	0.1-0.4	>2	$\leq$0.10	$\leq$0.07	$\geq$0.76	∿200	$\geq$60

Table (12) gives the names of the meteorites belonging to two subtypes.

TABLE 12

MEMBERS OF VIGARANO AND ORNANS

Vigarano subtype	Ornans subtype
Allende (Mexico)	Felix (Albania)
Bali (Cameron)	Kainsaz (U.S.S.R.)
Coolidge (Kansas)	Karoonda (Australia)
Efremorka (U.S.S.R.)	Lancé (France)
Grosnaja (U.S.S.R.)	Ornans (France)
Kaba (Hungary)	Warrenton (Missouri)
Leoville (Kansas)	
Mokoia (New Zealand)	
Vigarano (Italy)	

Thus we ultimately find the place of the Allende meteorite in the diversive classification of the meteorites. It is a carbonaceous chondrite of type III belonging to the Vigarano subtype. It has the Si/Mg ratio characteristic of the carbonaceous chondrites, and it falls within the range of other CIII meteorites. The conjunction of iron-poor olivine in chondrules with iron-rich olivine in matrix is also a distinctive characteristic for these meteorites. Its carbon content (.26%) is low for a carbonaceous chondrite, lower in fact than in a number of chondrites

whose Si/Mg ratio places them in the ordinary classes. The large size of its chondrules and some other specific properties place it in the Vigarano subtype.

6.4 STRUCTURE AND COMPOSITION OF THE ALLENDE

Allende meteorite is an unusually heterogeneous meteorite having complexity in its composition and structure. A comprehensive discussion of its diversive mineralogy and structure is beyond the scope of this work. However, an outline of this topic is given below.

A broken surface of a specimen of Allende meteorite shows a dark grey interior densely spotted with chondrules (spherical aggregates of silicate minerals averaging 1 mm in diameter) and with larger white and pink aggregates. A magnified picture of three slices taken from an Allende individual is shown in Fig. (11). Circular spots in the dark gray matrix are the chondrules. Over the surface several comparatively large irregular aggregates are also distinctly visible in the picture.

The bulk composition of Allende consists of 77 elements, many of them in the parts per million order (19). Of them, the dominating elements are, in decreasing order, O, Fe, Si, Mg, S, Ca, Aℓ, Ni, Cr, Na, C, Mn, P and Ti.

FIG. 11 Photograph of three slices taken from an Allende individual.

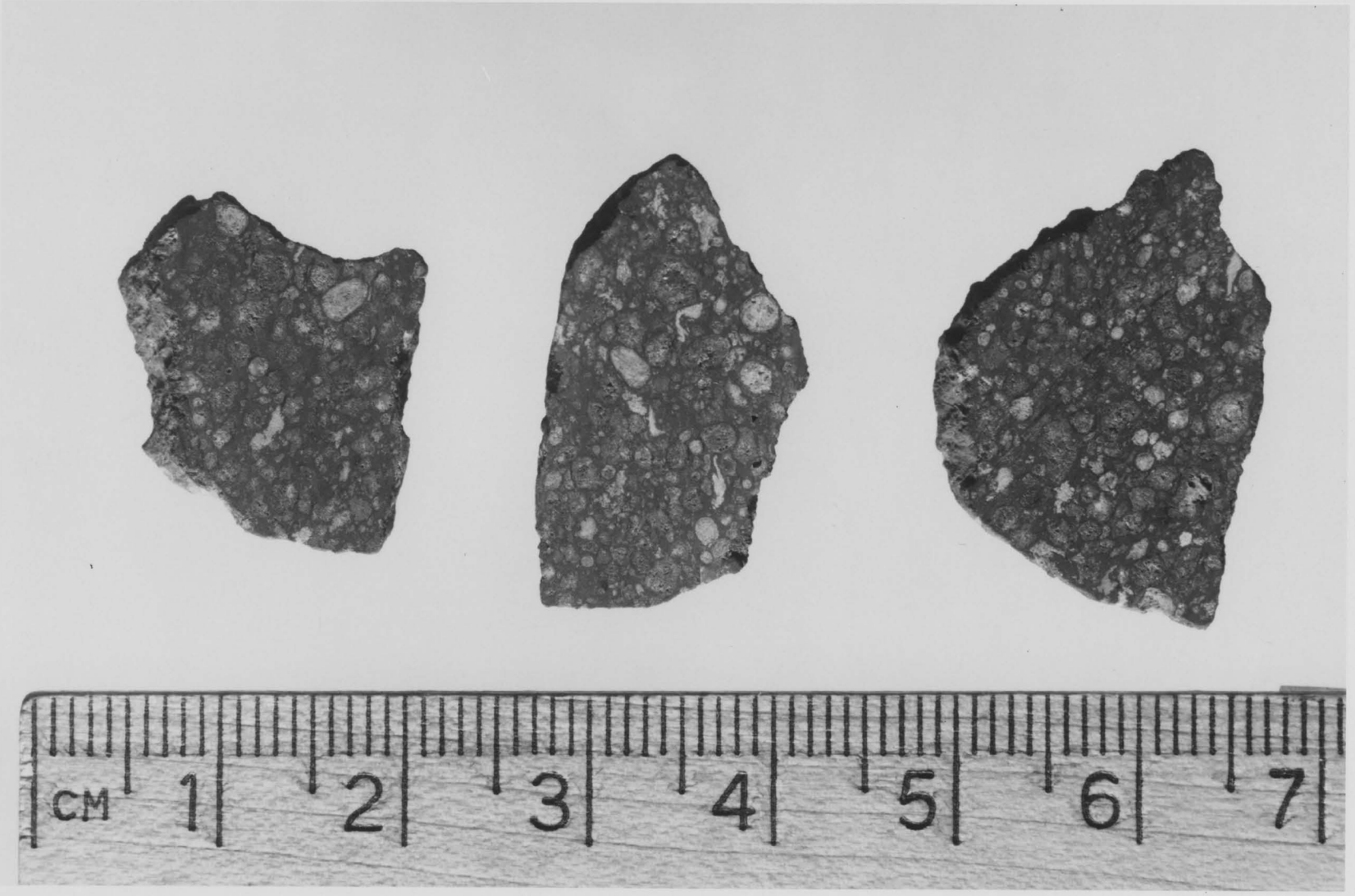
CM
1
2
3
4
5
6
7

Elements O, Fe, Si and Mg make up over 90% of the whole; these elements are present largely as olivine, $(Mg,Fe)_2SiO_4$.

The dark grey colour of the matrix is due to the presence of carbon. Allende has relatively low carbon content (.26%) for a carbonaceous chondrite, some of which contain 1% or more and all of the carbon is present in the matrix. The matrix consists of micron-sized crystals of olivine which are coated with a thin film of carbonaceous material consisting of high-molecular-weight organic polymers.

A list of the minerals with their sites in the Allende meteorite is given in table (13). Many of these minerals were not previously found in meteorites. Moreover, different components of the Allende have rather distinctive mineralogy (Table 13). Principal components with their volume percentage are:

(a) Matrix, largely of Fe-rich olivine (∿ 60%),

(b) Mg-rich chondrules (∿ 30%),

(c) Ca,Aℓ-rich chondrules (∿ 5%),

(d) Ca,Aℓ-rich aggregates (∿ 5%).

Among these Ca,Aℓ-rich chondrules and aggregates have much in common. The investigation of these

† TABLE 13

MINERALS IN THE ALLENDE METEORITE

Name	Formula	Matrix	Mg-rich chondrules	Ca,Aℓ-rich chondrules	Ca,Aℓ-rich aggregates
Kamacite	(Fe,Ni)		x		
Awaruite	$FeNi_3$	x	x		
Copper	Cu	x			
Troilite	FeS	x	x		
Pentlandite	$(Fe,Ni)_3S_8$	x	x		
Chromite	$FeCr_2O_4$	x			
Spinel	$MgAℓ_2O_4$			x	x
Hercynite*	$FeAℓ_2O_4$				x
Perovskite*	$CaTiO_3$			x	x
Hibonite*	$CaAℓ_{12}O_{15}$			x	
Olivine	$(Mg,Fe)_2SiO_4$	x	x	x	x
Enstatite	$MgSiO_3$				x
Clinoenstatite	$MgSiO_3$			x	

† Taken from Ref. (19)

* Mineral not previously found in meteorites

TABLE 13 (cont'd)

MINERALS IN THE ALLENDE METEORITE

Name	Formula	Matrix	Mg-rich chondrules	Ca,Aℓ-rich chondrules	Ca,Aℓ-rich aggregates
Clinohypersthene	$(Mg,Fe)SiO_3$	x			
Diopside	$CaMgSi_2O_6$			x	x
Fassaite*	$Ca(Mg,Aℓ,Ti)(Aℓ,Si)_2O_6$			x	x
Wollastonite*	$CaSiO_3$			x	
Anorthite	$CaAℓ_2Si_2O_8$			x	
Melite	$Ca_2(Mg,Aℓ)(Si,Aℓ)_2O_7$			x	x
Grossular*	$Ca_3Aℓ_2Si_3O_{12}$			x	x
Andradite*	$Ca_3Fe_2Si_3O_{12}$			x	
Rhënite*	$Ca_2Mg_3Ti_3Aℓ_4Si_2O_{20}$			x	
Nepheline	$NaAℓSiO_4$				x
Sodalite*	$Na_4Aℓ_3Si_3O_{12}Cℓ$				x
Cordierite*	$Mg_2Aℓ_4Si_5O_{18}$				x

* Mineral not previously found in meteorites

components has revealed a remarkable variety of chemical fractionations. For detailed discussions the reader is referred to B. Mason (19) and Clarke et al. (18).

6.5 ISOTOPIC ANOMALIES IN THE ALLENDE METEORITE

The meteorites are our best source of information concerning the earliest history of the solar system. Isotopic variability in them has contributed significantly to our knowledge in this area. Terrestrial and lunar materials provide a baseline relative to which we may observe variability in the meteorites.

Isotopic abundance variations have been detected in many meteorites but it is in the carbonaceous chondrites in which they are most clearly seen. Variations in isotopic abundances are brought about by a number of processes such as mass-fractionation or the creation or destruction of isotopes in nuclear reactions, including both radioactive decay and energetic particle reactions. Radioactive decay is effective in modifying the isotopic abundances of the elements that are daughter products not only of long-lived parents still present (e.g. ^{238}U, ^{235}U, ^{232}Th, ^{147}Sm, ^{87}Rb, ^{40}K) but also of extinct radionuclides

(e.g. ^{244}Pu, ^{129}I, $^{26}A\ell$). After liberation from their parent bodies, the meteorites are exposed to the galactic cosmic radiation for a period of 10^6 to 10^9 years, during which time substantial quantities of cosmogenic nuclides, both stable and radioactive are produced by spallation reactions. If at any time in its history, an extraterrestrial object is exposed to the solar wind, its surface acquires an implanted solar component, which may have been isotopically modified by nuclear reactions in the sun. Gaseous diffusion which is essentially a mass-dependent fractionation process is mainly responsible for isotopic anomalies in noble gases. In addition, there are a number of isotopic variations which cannot be accounted for in terms of the known solar system processes, and they might have originated from presolar nucleosynthesis.

In the Allende meteorite isotopic anomalies have been observed for many elements both in the bulk material and in the so called high condensation temperature inclusions. The searches for anomaly have been carried out since 1972 (42), by many groups of scientists of different countries, mostly by the method of mass spectrometry. Up until the present time, there have been reports of

anomalies in the isotopes of various elements. Elements in Allende for which mass dependent variations and nuclear anomalies have been confirmed are (42 and 52)

Oxygen	Calcium	Samarium
Neon	Krypton	Uranium
Magnesium	Strontium	Tellurium
	Xenon	
Silicon	Barium	
Sulphur	Neodymium .	

6.6 THE ABUNDANCES OF THE STABLE ISOTOPES OF IRON

This work presents the first evidence of an isotopic anomaly in iron from the Allende meteorite. There has been very little work (33 to 39) on the mass spectrometry of iron since the days (1930 - 1950 roughly speaking) when the relative abundances of the stable isotopes of all the elements were being determined. Since 1950 the elements which have been most studied mass spectrometrically fall into four main classes:

1) light elements
2) rare gases
3) fission products
4) Pb, Sr, Ar.

Light elements such as H, C, N, O, S have been widely studied in stable isotope geochemistry where the variations of their isotope abundances have been used as tracers of geochemical and biological processes. All of the named elements can be analysed in gas source mass spectrometers which by their nature permit the detection of very small differences in isotopic abundances.

The rare gases have been extensively studied in terrestrial, meteoritic and lunar samples as well as in the solar wind and the atmosphere of Mars and Venus. Because of their lack of chemical interactions and the large number of stable isotopes in Kr and Xe they are sensitive probes of physical, nuclear and astrophysical processes.

Fission products, whether they be analysable as solids or gases, have been studied in order to elucidate the fission process.

Elements which are implicated in radioactive decay chains which have half-lives long enough to apply to geochronological processes have been extensively studied.

Iron falls into none of the above categories, and in consequence, following the early survey work it appears to have been virtually ignored. However there are two factors which make iron a promising candidate for a programme of isotope geochemical investigation:

1) Iron occurs in two oxidation states and it has four stable isotopes covering a mass range from 54 to 58. This suggests that changes in isotope abundances should occur and should be detectable in the geochemical cycling of the element.

2) Iron occurs near the peak of binding energy and this suggests that interesting effects could be present in those meteorite samples which have been shown to display isotopic anomalies in other elements which are indicative of the imperfect mixing in the early solar system of materials which have had widely differing nucleosynthetic histories.

In 1948, J.R. White and A.E. Cameron (33) published the results of their determination of the natural

abundances of iron isotopes. These measurements used $FeCl_2$ which was vapourised and then ionised by electron bombardment to produce Fe^+ ions. The relative abundances which they determined were not corrected for systematic effects in the mass spectrometer and the possibility of variable isotope abundances in nature was not investigated. Perhaps the only recent report on iron isotope abundance determinations is that in Ref. (40) which was evidently an unsuccessful attempt to run iron in a conventional gas source mass spectrometer in order to study possible terrestrial isotope abundance variations. $Fe(CO)_5$ forms a layer in the mass spectrometer inlet tube causing memory peaks with intensities camparable to those of the new sample. The problem with iron and some other elements like platinum, tungsten, and palladium is that they cannot be ionised efficiently. So, in the case of the ionisation of iron a comparatively large amount of its compound has to be used; while for most of the other elements a quantity of the order of micrograms, or even nanograms, suffices.

CHAPTER 7

EXPERIMENT

7.1 THEORY

Neutron capture gamma-ray analysis can be used to investigate iron isotope abundance variations for the two isotopes, ^{56}Fe and ^{54}Fe. The iron doublet at 7.64 MeV is due to the de-excitation of ^{57}Fe following its creation from thermal neutron capture by ^{56}Fe. Another line at 9.3 MeV energy is due to the transition in ^{55}Fe created by $^{54}Fe(n,\gamma)^{55}Fe$ reaction.

From equation (3,4), we know that for a given sample with n_i atoms of isotope i, the observed intensity of the γ-rays of energy E_j is

$$R_{ij} = I_{ij}\varepsilon(E_j)\frac{n_i}{v}\sigma_i\phi'' \int_v \phi(\vec{r})d^3\vec{r} \qquad (3.4)$$

in which self-absorption has been neglected. But as the isotopic variation effect may be very small, we should investigate if self-absorption is significant.

In Fig. (12), the activity at P is $\rho dxdy$ where ρ is the activity density. The number of photons which leave is then $\rho e^{-\mu(L-x)}dxdy$ where L-x is the distance

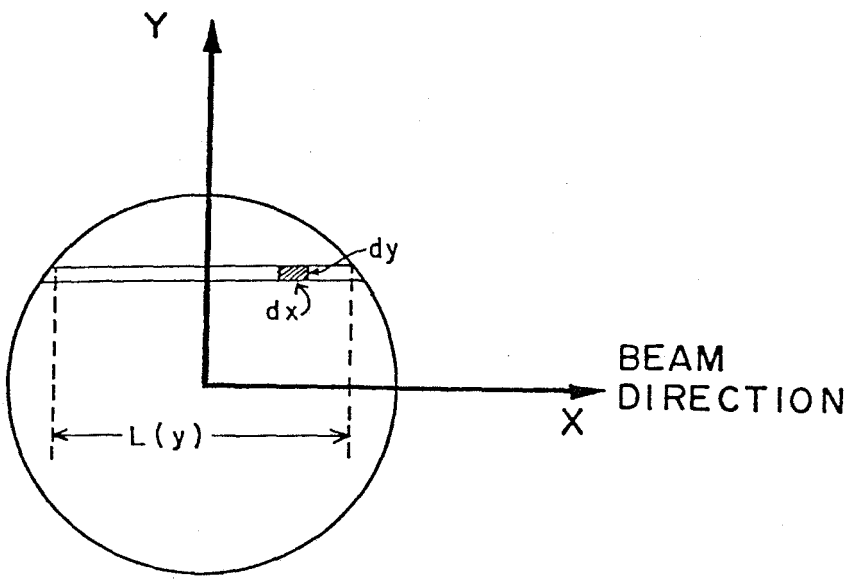

FIG. 12 DIAGRAM FOR SELF ABSORPTION

from P to the perimeter. The escape probability is thus

$$Pe = \frac{\iint e^{-\mu(L-x)}\,dxdy}{\iint dxdy}$$

$$= \frac{\int (1-e^{-\mu L(y)})\,dy}{\mu A}$$

where A is the area and L(y) is the chord length. Note that $A = \int (L(y)dy$. Expanding to the second order

$$1-e^{-\mu L} = \mu L - \frac{\mu^2 L^2}{2}, \text{ so that}$$

$$Pe = 1 - \frac{\mu}{2A}\int L^2(y)dy \qquad (7.1)$$

For a circular cross-section $L^2(y) = 4(R^2-y^2)$

$$Pe = 1 - \frac{2\mu}{\pi R^2}2\int_{-R}^{R} (R^2-y^2)dy$$

$$= 1 - \frac{8\mu R}{3\pi} = 1-\mu t \qquad (7.2)$$

where $t = \frac{8R}{3\pi} = 0.40$ cm for our capsules. For $\rho = 5.2$ g/cm^3, the maximum Fe_2O_3 density (53), $\mu = 0.1446$ cm^{-1} and 0.1414 cm^{-1} for 7640 keV and 9300 keV respectively (54).

Using these values of μ in eqn. 7.2 the escape probability for 7640 keV γ-ray is .942 and that for 9300 keV is 0.943. The escape probabilities differ by 0.1%.

Thus it is found that the self-absorption factor is really negligible. Now referring subscripts 1 and a to the isotope ^{56}Fe and the doublet, and 2 and **b** to the isotope ^{54}Fe and 9.3 MeV line, for a particular spectrum, it follows from equation (3.4) that

$$R_{1a} = \frac{n_1}{v} I_{1a}\varepsilon(Ea)\phi'' \sigma_1 \int_v \phi(\bar{r})d^3\bar{r}$$ area of doublet per unit time,

and

$$R_{2b} = \frac{n_2}{v} I_{2b}\varepsilon(E_b)\phi'' \sigma_2 \int_v \phi(\bar{r})d^3\bar{r}$$ area of 9.3 MeV peak per unit time.

From these two equations,

$$\frac{R_{2b}}{R_{1a}} = \frac{n_2}{n_1} \frac{I_{2b}\varepsilon(E_b)\sigma_1}{I_{1a}\varepsilon(E_a)\sigma_2} \qquad (7.3)$$

Alternate analysis of a sample with a standard material under constant experimental conditions gives by eqn. (7.3),

$$\frac{(R_{2b}/R_{1a})_{unknown}}{(R_{2b}/R_{1a})_{standard}} = \frac{(n_2/n_1)_u}{(n_2/n_1)_{st.}} = \frac{(^{54}Fe/^{56}Fe)u}{(^{54}Fe/^{56}Fe)st.} \qquad (7.4)$$

Define the quantity $\delta^{54}Fe$ as

$$\delta^{54}Fe\% = \left[\frac{(^{54}Fe/^{56}Fe)u}{(^{54}Fe/^{56}Fe)st.} - 1\right] \times 100, \qquad (7.5)$$

the fractional difference in the isotope ratio $^{54}Fe/^{56}Fe$ for an unknown sample relative to a standard material.

7.2 INTERFERENCE

If the isotopic anomaly is very small, particular care should be taken so that there is no interference in the 7640 keV and 9300 keV peaks. It was checked in section 3.3.1 that there is no appreciable interference at 7640 keV. From the literature survey it was also found there is no line under the 9300 keV peak. However, since there are multitude number of wide variety of elements in the meteorite, some unknown line might boost the anomaly. The first argument is that although another meteorite Bruderheim, as shown in table (14) contains similar elements in a comparable amount, anomaly was not

TABLE 14

COMPARISON OF ALLENDE AND BRUDERHEIM METEORITES

Element	Approximate amount in percent in Allende (A)	Approximate amount in percent in Bruderheim (B)	A/B
Si	14.49	25.45	0.57
Mg	12.85	15.05	0.85
Fe	24.80	22.70	1.09
Aℓ	1.53	0.98	1.56
Ca	2.00	1.24	1.61
Na	0.45	0.75	0.60
K	0.01	0.11	0.09
Ti	0.10	0.07	1.43
Mn	0.11	0.26	0.42
Ni	1.10	1.30	0.85
Cr	0.32	0.41	0.78
C	0.27	0.04	6.75
Co	0.79	0.05	15.80

found in it. Although the table is not exhaustive and its values are approximate, it definitely adds to our confidence. Finally, almost all the iron in the form of Fe_2O_3 was extracted from the Allende sample and was run. The tedious and complicated process of extraction was kindly carried out by Mr. J. Monster and Dr. C.E. Rees.

Another possibility of interference is the container itself. Both the beryllium and graphite capsules contain minute amounts of natural iron. However, since the amount of iron in both of them is of the order of ppm, it will not affect the results significantly.

7.3 PROCEDURE

As the terrestrial standard we used Fe_2O_3 and Fe_3O_4 and as extra-terrestrial, Allende meteorite and moon rock. In table (15) there are given the amounts of the samples, hour of run and types of container used. Also included in the table is Bruderheim and Allende chip which was measured earlier in this laboratory (20). Fe_2O_3 extracted from Allende meteorite is named Allende iron in the table.

TABLE 15

DATA FOR STANDARDS AND UNKNOWNS

Name of sample	Physical Form	Approx. amount taken in gm	Approx. amount of iron in gm	Hour of run	Capsule used as container
Allende	Powder	.9	.22	127	Be
Fe_3O_4	Powder				C
Allende	Powder	.9	.22	48	Be
Fe_2O_3	"	.6	.42	65	Be
Allende iron	"	.62	.43	62	C
Fe_2O_3	"	.50	.35	96	C
Allende iron	"	.62	.43	20	C
Fe_2O_3	"	.50	.35	23	C
Allende	Chip				
Bruderheim	Chip				
Moon rock	Chip	1.2		212	Be
Fe_3O_4	Powder				
Moon rock	Chip	1.2		260	Be
Fe_2O_3	Powder	.6	.42	65	Be

Recently, with a new intrinsic Ge detector (28.3 cm^3 active volume; fabricated by Princeton Gamma-Tech Inc.) in the pair spectromater and with reactor power at 2 MW thermal, double the power used for all runs in this work, a new series of experiments were carried out. This time the meteorite iron runs were alternated with the natural iron runs. These runs were integrated to give a single pair and the $\delta^{54}Fe\%$ value was determined from it. The facts regarding these runs are given in table (16).

TABLE 16

DATA FOR A STANDARD AND METEORITE IRON

Natural Fe_2O_3 in C capsule			Meteorite Fe_2O_3 in C capsule		
Physical Form	Amount taken in gm	Hour of run	Physical Form	Amount taken in gm	Hour of run
Powder	.6185		Powder	.6217	
		20			
		24			47
		46			35
Total:		90			82

7.4 RESULTS

The various values of δ obtained from different pairs of standard and unknown are given in table (17) and (18). The last value in table (17) is corresponding to runs of table (16).

TABLE 17

VALUES OF $\delta^{54}Fe\%$ FOR THE ALLENDE

Sample	Ratio of areas of the peaks due to ^{54}Fe and ^{56}Fe.	$\delta\ ^{54}Fe\%$
Allende Fe_3O_4	.05676 ± .0002 .05583 ± .0005	1.64 ± .9
Allende Fe_2O_3	.05477 ± .00051 .05369 ± .00024	2 ± 1
Iron extracted from Allende Fe_2O_3	.05475 ± .00027 .05418 ± .00024	1.05 ±.6
Iron extracted from Allende Fe_2O_3	.05420 ± .0004 .05337 ± .00042	1.55 ± 1
Allende Bruderheim		1.14 ± .66
Iron extracted from Allende Fe_2O_3	.05826 ± .00030 .05657 ± .00028	3.0 ± .7
Average		1.7 ± .3

TABLE 18

VALUES OF $\delta^{54}Fe\%$ FOR LUNAR SAMPLE

Sample	Ratio of areas of the peaks due to ^{54}Fe and ^{56}Fe	$\delta^{54}Fe\%$
Moon rock Fe_3O_4	.05581 ± .00032 .05583 ± .0005	0 ± .9
Moon rock Fe_2O_3	.05400 ± .00040 .05369 ± .00024	.6 ±.8
Average		.3 ±.6

7.5 DISCUSSIONS OF RESULTS

In table (17) a distinct effect is observed in the Allende meteorite. Normalisation of Allende value to Bruderheim was done by Prestwich. This, however, is added in table (17) because this δ value is in harmony with other δ values. It is also obvious from table (18) that there is no isotopic anomaly of iron in the moon rock. The very small δ value that is obtained is masked by error and it can well be presumed that it is essentially zero.

Taking terrestrial Fe_2O_3 or Fe_3O_4 as the standard

there is definitely a positive anomaly in $^{54}Fe/^{56}Fe$ ratio in Allende meteorite, as is apparent from fig. (13). Though the errors in $\delta^{54}Fe\%$ are quite large, the values themselves are on the positive side. The mean value for $\delta^{54}Fe$ is 1.7 ± .3%. This amount of anomaly is significant. But unfortunately this work leaves some of the points questionable. For example, in the first place, we did not take any sample other than laboratory-made Fe_2O_3 or Fe_3O_4. We do not know at this stage if there is variation in iron isotopic ratio of different compounds and of same or different compounds from different terrestrial sources, in which presumably different chemical processes occurred. In other words, nothing can be said as to if there is any mass fractionation in terrestrial iron. Thus we lost the generality by linking to only two terrestrial irons. In the second place, unfortunately, this method does not permit us to look at some other isotope of iron effectively. There is, however, one peak due to ^{57}Fe at 8.37 MeV. But not only the partial cross-section for the transition in this line is very small, the natural abundance of ^{57}Fe is about 3 times less than even that of ^{54}Fe which itself has low abundance. With the system it is not possible

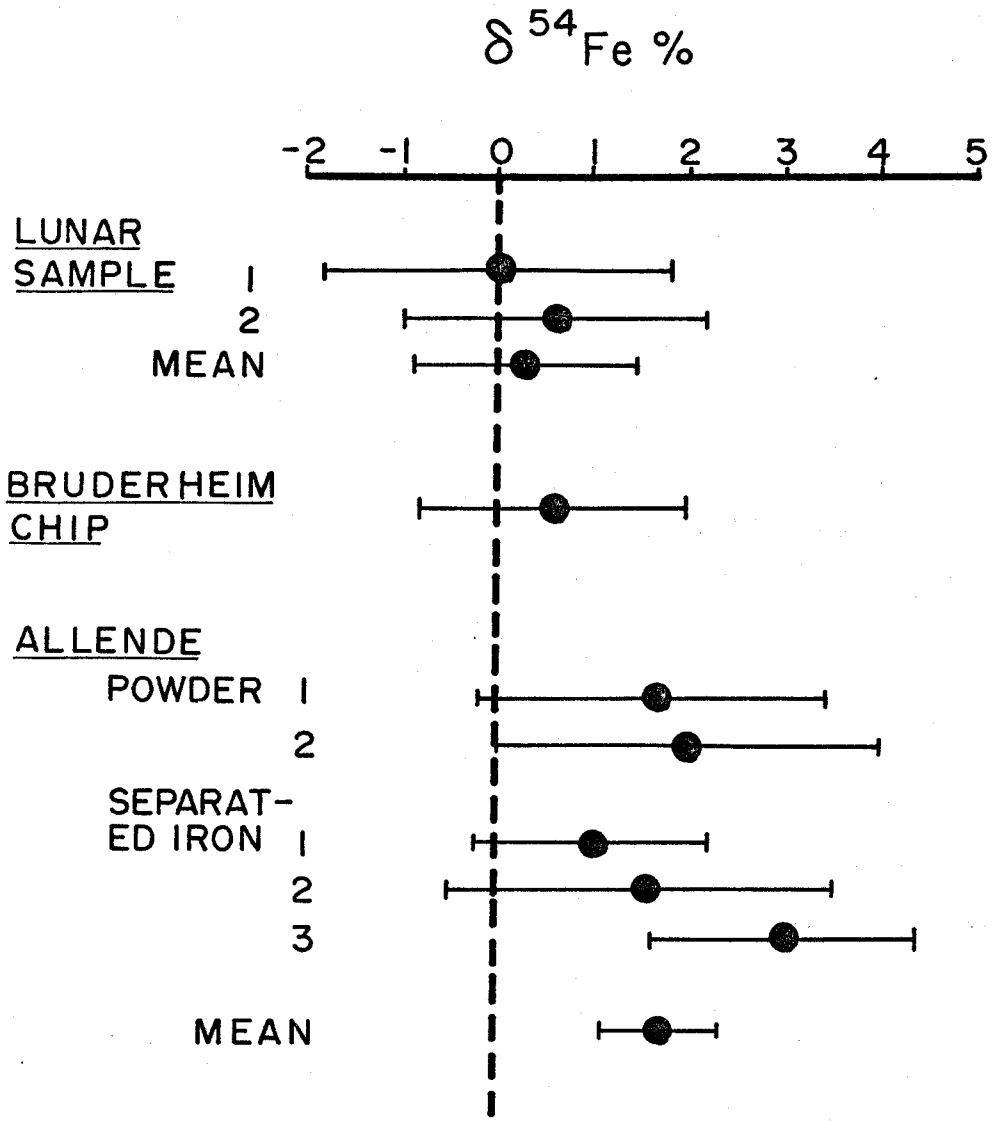

(ERROR BARS ARE ± 2σ)

to accumulate a sufficient statistical sampling in a reasonable counting period.

TABLE 19

VALUE OF δ^{57}Fe% FOR THE ALLENDE

Sample	Ratio of areas of the peaks due to ^{57}Fe and ^{56}Fe	δ^{57}Fe%
Iron extracted from Allende	.0031 ± .00006	3.3 ± 2.6
Fe_2O_3	.0030 ± .00006	

The δ^{57}Fe% value has so large an error that we cannot definitely infer anything from it. However, had there been a few more values even with this large error at our disposal, we could at least observe the trend of the values.

Broadly and rather generally speaking the isotopic anomaly of iron may have either chemical or nuclear origin. If the δ^{54}Fe% value be positive the δ^{57}Fe% value should

be negative and numerically half the former in the case of some chemical origin. But if both of them are positive or they are opposite in sign but do not obey the mass difference rule, then it implies some nuclear origin whatever its nature be.

The argument against the fact that various natural iron compounds were not used is dampened at least partially, by the presence of the data relating to the moon rock and Bruderheim in which a similar effect was not observed.

CHAPTER 8

CONCLUSIONS

In the first part of this work, S/Si and Fe/Si ratios were determined for the Allende and the lunar samples. The values obtained for the Allende agreed well with those available in the literature. The main problem was to determine the S/Si value for the lunar sample as there were discrepancies among the existing values in the literature. This value as obtained in this work agreed within error with those of Rees et al. and thus resolved the contradiction in the literature. With higher reactor power and better resolution of the detector the value can be determined with greater precision and the values for other elements in the samples can also be determined efficiently with Neutron Capture Gamma Ray Analysis.

In the second part, evidence has been found for the isotopic anomaly in iron from the Allende meteorite. This may have significant implication in the early history of the solar system formation. The δ^{54}Fe value with respect to ^{56}Fe has been found to be 1.7 ± .3%.

With the method of NCGA, δ value cannot be determined for ^{57}Fe and ^{58}Fe and thus it cannot be inferred at this point if this anomaly is of nuclear or chemical origin. Neutron Activation Analysis may be a complementary method for this problem. The nuclear reactions $^{54}Fe(n,p)^{54}Mn$ and $^{58}Fe(n,\gamma)^{59}Fe$ may be resorted to for determining $\delta^{54}Fe$ with respect to ^{58}Fe with NAA method. Proton activation analysis by (p,n) reactions may also be tried for determining $\delta^{57}Fe$ and $\delta^{58}Fe$ both with respect to ^{56}Fe. By carrying out the same experiments with different compounds of various origins as standard, the isotopic variations in terrestrial iron itself can be probed.

BIBLIOGRAPHY

(1) C.E. Rees, H.G. Thode, Proc. Lunar Sci. Conf. 5th (1974) p. 1963.

(2) Gibson et al., Lunar Science V (1974) p. 267, Lun. and Plan. Inst., Houst.

(3) G. Shani, D. Cohen, Int. J. App. Rad. Iso. 27 (1976) 349.

(4) G.A. Bartholomew, L.A. Higgs - AECL - 669 (1958) pp. 145.

(5) L.V. Groshev et al., Atlas of Thermal neutron capture gamma rays, Atomizdat, Moscow (1958).

(6) G. Van Middelkoop, H. Greppeluar, Nucl. Phys. 80 (1966) 321.

(7) E.T. Jurney et al., Anal. Chem., 46 (1974) 1223.

(8) D.A. Fay et al., J. Radioanal. Chem. 43 (1978) 263.

(9) N.C. Rasmussen, Y. Hukai, Trans. Am. Nuc. Soc., 10 (1967) 29.

(10) N.C. Rasmussen, Analysis Instrum., 7 (1969) 186.

(11) N.C. Rasmussen, Trans. Am. Nu. Coc., 14 (1971) 931.

(12) D.R. Parsignault et al., AEC Report CONF. 710402, vol. III session IV, p. 40.

(13) A.E. Profio et al., Anal. Chem., 46 (1974) 1223.

(14) A.H. Colenbrander, T.J. Kennett, Nucl. Intr. Methods 116 (1974) 251.

(15) A. Robertson et al., Nucl. Instr. Methods 127 (1975) 373.

(16) N.C. Rasmussen et al., Thermal Neutron Capture Gamma Ray Spectra of the elements, MITNE-85, MIT, Cambridge, Mass., 1969.

(17) P.R. Bevington, Data reduction and error analysis for the physical sciences, McGraw-Hill Book Co., 1969, p. 250.

(18) Clarke et al., Smithson. Contr. Earth. Sci., 5 (1970) pp 53.

(19) B. Mason, Acc. of Chem. Res. 8 (1975) 217.

(20) W.V. Prestwich, private communication.

(21) Y. Harry et al., Geochim. Cosmochim. Acta, 41 (1977) 1145.

(22) T.S. McCarthy, L.H. Ahreno, Earth Planet Sci. Lett. 14 (1972) 97.

(23) King et al., Science 163 (1969) 928.

(24) J.F. Kerridge, personal communication, noted in (1).

(25) Moor et al., Lunar Science V (1974) p. 520, Lun. Plan. Ins., Houst.

(26) Gibson et al., Lunar Science V (1974), p. 267, Lun. Plan. Ins., Houst.

(27) H. Wanke et al., Proc. Lunar Sci. Conf. 6th (1975) 1313.

(28) LSPET, Science, 182 (1973) 659.

(29) J.M. Rhodes et al., Lun. Sci. Conf. 5th (1974) 1097.

(30) H.B. Wiik, Geochim. Cosmochim. Acta, 9 (1956) 279.

(31) W.R. Van Schmus et al., Geochim. Cosmochim. Acta, 31 (1967) 747.

(32) J.T. Wasson, Meteorite Classification and Properties, Springer-Verlag Berlin, Heidelberg, New York (1974) p. 23.

(33) J.R. White and A.E. Cameron, Phys. Rev., 74 (1948) 991.

(34) Aston, Nature 133 (1935) 684.

(35) Aston, Proc. Roy. Soc. A49 (1935) 396.

(36) A.O. Nier, Phys. Rev. 55 (1939) 1143.

(37) G.E. Valley and H.H. Anderson, Phys. Rev. 59 (1941) 113.

(38) G.E. Valley and H.H. Anderson, J. Am. Chem. Soc. 69 (1947) 1871.

(39) R.F. Hibbs, AECU - 556 (1949).

(40) I.P. Shadokii, Zb. Fiz. Khim., 49 (1975) 52.

(41) E.M. Pell, J. Appl. Phys. 31 (1960) 291.

(42) R.N. Clayton et al., Science 182 (1973) 485.

(43) S.P. Smith et al., Geochim. Cosmochim. Acta, vol. 41, No. 5 (1977) 627.

(44) Typhoon Lee et al., Geophys. Res. Lett., vol. 3, No. 2 (1976) 109.

(45) Clayton et al., Proc. Lunar Sci. Conf. 9th (1978) 1267.

(46) C.E. Rees, H.G. Thode, Geochim. Cosmochim. Acta 41 (1977) 1697.

(47) Typhoon Lee et al., Astr. Jour. (letters) vol. 220, No. 1, part 2 (1978) p. L21.

(48) D.A. Papanastassion et al., Geoph. Res. Lett. vol. 5, No. 7 (1978) p. 595.

(49) M.T. McMulloch et al., Astr. Jour. (letters) vol. 220, No. 1, part 2 (1978) p. L15.

(50) M.T. McMulloch et al., Geophys. Res. Lett. vol. 5, No. 7 (1978) 599.

(51) J.W. Arden, Nature 269 (1977) 788.

(52) R.V. Ballard et al., Nature 277 (1979) 615.

(53) R.C. Weast, CRC Handbook of Chemistry and Physics, 59th ed., Chemical Rubber Publishing Co., 1978.

(54) E. Storm and H.I. Israel, Nuclear Data Tables, A7 (1970) 565.